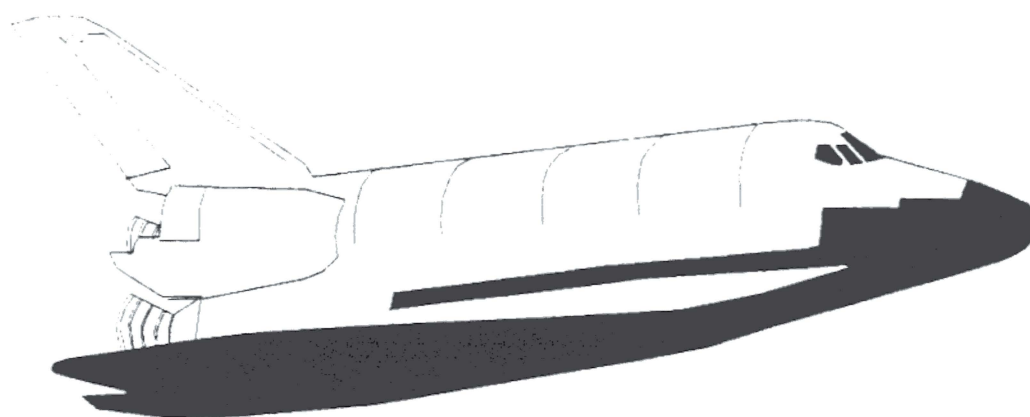


Orbiter Avionics Radiation Handbook

Orbiter and GFE Projects



September 30th, 1999



National Aeronautics and
Space Administration

Lyndon B. Johnson Space Center
Houston, Texas

REVISION AND HISTORY PAGE

REVISION	DESCRIPTION	PUB. DATE
----	Baseline Issue	01-17-1989
A	Modified Section 3 to allow qualification of EEE parts using high energy and heavy ion testings.	09-30-1999

FORWARD

When the Orbiter was designed, there was little need to be concerned about the effects of ambient ionizing radiation on the performance and reliability of electronic hardware. Subsequent trends in electronic parts are toward smaller feature size, higher densities, and lower power. These parts are superior in ordinary environments, but may evidence increased susceptibility to radiation effects.

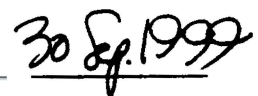
This handbook was assembled to document the radiation environment for design of Orbiter avionics. It also maps the environment through vehicle shielding and mission usage into discrete requirements such as total dose. Some details of analytical techniques for calculating radiation effects are provided. It is anticipated that appropriate portions of this document will be added to formal program specifications.

The Orbiter Avionics Radiation Specification Working Group was formed by the Orbiter Avionics Systems Office in November 1987. This group was commissioned to develop the fundamental methodology of this handbook. Appendix E lists the members of this working group who each contributed to this handbook. The original handbook was prepared by McDonnell Douglas Astronautics Company – Engineering Services, Houston, Texas. It was submitted to the National Aeronautics and Space Administration, Lyndon B. Johnson Space Center in response to Contract NAS9-17650, Task Order VA88012.

The original version of the handbook relied heavily on low energy, heavy ion testing of individual components. However, since 1995 high energy testing with protons and/or heavy ions has become more practical. Therefore, the handbook revision in September 1999 allows high energy testing for system or part qualification. Note that this revision does not prohibit individual component testing at low energy, it simply provides an additional option for qualifying devices.



Pat M. O'Neill, Ph.D.
Technical Manager Radiation Effects
NASA/JSC Engineering Directorate



Date

TABLE OF CONTENTS

<u>PARAGRAPH</u>	<u>PAGE</u>
FORWARD.	ii
TABLE OF CONTENTS.	iii
LIST OF TABLES	
LIST OF FIGURES	vii
INTRODUCTION	
Objective and Scope	
1.2 Applicability	1-
3 Requirements for Resistance to the Effects of Radiation ..	
1.3 Single Event Upsets ...	1-1
.3.2 Latchup	-2
.3.3 Total Dose Effects.	
1.4 Design Acceptance Criteria	1-2
1.4.1 MTBF Definitions....	1-2
1.4.2 Acceptance Criteria.	-3
5 Further Considerations	1-3
2 RADIATION ENVIRONMENT	
2.1 Natural Radiation Environment	2-1
2.2 Single Event Effect Environment	
2.2.1 Direct Deposition by Ions	2-1
2.2.2 Nuclear Reactions Caused by Protons	2-3
2.3 Total Dose Effect Environment ..	2-8
2.4 Environment Error Analysis ..	

TABLE OF CONTENTS

<u>PARAGRAPH</u>	<u>PAGE</u>
3 QUALIFICATION OF ELECTRONIC COMPONENTS AND SYSTEMS.....	3-1
3 Introduction...	
3.2 Single Event Effect Testing of Electronic Components	3-
3.2 Low Energy Heavy Ion Testing	3-1
3.2.2 High Energy Proton Testing	3-2
3.2.3 High Energy Heavy Ion Testing	3-3
3.3 Total Dose Testing....	3-4
3.4 Conclusion	
REFERENCES	
APPENDICES	
A SINGLE EVENT RATE CALCULATIONS	A-
A. Background Theory	A-
A. Charged Particle Environment.	A-1
A.1.2 Device Characteristics for Bit Errors	A-2
A.1.3 Upset Rate Formulation	A-3
A.1.4 Experimental Threshold LET.....	
A.1.5 Dimensions of the Sensitive Region	A-5
A.2 Greatest Upper Bound (GUB) on Upset Rate	A-9
A.3 SEU Rate Calculation	A-11
A.4 Proton Induced Upset Rate	A-13
A.5 Latchup	A-17
B SINGLE EVENT EFFECT SENSITIVITY ANALYSIS	

TABLE OF CONTENTS

<u>PARAGRAPH</u>	<u>PAGE</u>
B.1 Height and Aspect Ratio	.B-
B.2 Fractional Live Time...	
B.3 Multiple Sensitive Volumes per Bit	
C PART RELIABILITY AND SINGLE EVENT EFFECT CALCULATION EXAMPLE.....	..C-1
D RADIATION ENVIRONMENT TABULATION	
D.1 Trapped Radiation....	D-1
E ORBITER AVIONICS RADIATION SPECIFICATION WORKING GROUP MEMBERS	E-1
F GLOSSARY/ACRONYMS.....	

LIST OF TABLES

<u>TABLE</u>		<u>PAGE</u>
2.3-1	Dose rate for each location for each orbital inclination	
2.3-2	Total dose exposure expected for Orbiter Avionics at each location... 2-9
A.3-	SEU rate coefficient versus threshold LET for the 90 degree orbit and 90% worst case interplanetary weather condition.....	
A.4-1	Equations for determining proton induced upset rates.	
D.1-	Tabulation of data plotted in Figure D.1-1. Trapped proton spectra contribution to radiation environment (unshielded). Orbit averaged for 28.5, 57, 90 degree orbits passing through the South Atlantic Anomaly	D-4
D.1-2	Tabulation of data plotted in Figure D.1-2. Trapped electron spectra contribution to radiation environment (unshielded). Orbit averaged for 28.5, 57, 90 degree orbits passing through the South Atlantic Anomaly	D-5

LIST OF FIGURES

<u>FIGURE</u>	<u>PAGE</u>
Integral LET (silicon) spectra for Internal location (MDM FA-1) for 90% worst-case (M=3, z=1 to 92) cosmic rays including trapped protons (AP8-MIN with 1965 IGRF magnetic field and 1964 epoch)	2-4
Integral LET (silicon) spectra for Free Space location (100 mil Al) for 90% worst-case (M=3, z=1 to 92) cosmic rays including trapped protons (AP8-MIN with 1965 IGRF magnetic field and 1964 epoch) ...	2-5
Orbiter location chosen for definition of internal radiation environment	2-6
Ray distribution versus thickness of aluminum for Internal Orbiter location (MDM FA-1).....	2-6
Differential energy spectra for Free Space location (100 mil Al) for 90% worst-case (M=3, z=1) cosmic ray protons including trapped protons (AP8-MIN with 1965 IGRF magnetic field and 1964 epoch)	2-7
Total, integral proton fluence for August 1972 solar proton event according to King (1973).....	2-10
Integral LET (silicon) spectra for Free Space location (100 mil Al) for August 1972 solar flare (M=9, z=1 to 92) and 90% worst-case (M=3, z=1 to 92) cosmic rays including trapped protons (AP8-MIN with 1965 IGRF magnetic field and 1964 epoch).....	2-13
2.4-2 Integral LET (silicon) spectra for Free Space location (100 mil Al) for August 1972 solar flare (M=9, z=1 to 92) and 90% worst-case (M=3, z=1 to 92) cosmic rays without including trapped (Van Allen) protons.....	2-14
A The stopping power (or LET) versus energy per atomic mass unit for a variety of ions. Taken from Adams (1986).....	A-7
A -2 Illustration of ion passing through the sensitive region of a semiconductor	A-8
A -3 Diagram illustrates the dependence of the upset cross section on the LET of the incoming ions	A-8

LIST OF FIGURES

<u>FIGURE</u>		<u>PAGE</u>
A.2-	Plot illustrating the dependence of error rate coefficient on the threshold LET	A-10
A.3-	Diagram illustrates the steps required to compute the greatest upper bound on the SEU rate	A-12
A.3-2	Parametric analysis to determine the maximum physically realizable upset rate of a part.....	A-12
A.4-1	Proton induced upset rates, quiet conditions, internal location at 28, 57, and 90 degrees.....	A-15
A.4-2	Proton induced upset rates, quiet conditions, free space location at 28, 57, and 90 degrees.....	A-15
A.4-3	Proton induced upset rates, flare conditions, internal location, at 28,57 and 90 degrees.....	
A.4-4	Proton induced upset rates, flare conditions, free space location, at 28, 57, and 90 degrees.....	A-16
A.5-1	Differential energy spectra for 90% worst-case (M=3) for 28.5 degree inclination orbit for hydrogen (u=1) and iron (u=56) cosmic rays for 100 mil Al and 5.0 inch Al shielding. Typical Tandem Van de Graaff spectra is shown for comparison.....	A-19
A.5-2	Differential energy spectra for 90% worst-case (M=3) for 90 degree inclination orbit for hydrogen (u=1) and iron (u=56) cosmic rays for 100 mil Al and 5.0 inch Al shielding.....	A-20
B.1-	Comparison of the actual and upper bound SEU rates versus depth	.B-3
B.1-2	Comparison of the actual and upper bound SEU rates versus aspect ratio	.B-4
D.1-	Trapped proton spectra contribution to radiation environment (unshielded). Orbit averaged for 28.5, 57, 90 degree orbits passing through the South Atlantic Anomaly.....	D-2
D.1-2	Trapped electron spectra contribution to radiation environment (unshielded). Orbit averaged for 28.5, 57, 90 degree orbits passing through the South Atlantic Anomaly.....	D-3

SECTION GENERAL

1.1 Objective and Scope

The objective of this handbook is to provide a source of natural radiation information and requirements for use by the Orbiter and GFE Projects and their contractors. A further objective is to document the origin of the data provided herein for traceability. Traceability is achieved with explanations in the text, references, and a record of those persons who contributed.

The scope includes definition of the radiation environment, structural shielding, effects on electronics, and preferred analytical methods.

2 Applicability

These requirements are applicable to all flight avionics hardware procured by the Orbiter and GFE Projects after the effective date of this document. However, formal contractual requirements are established by the device end item specification.

1.3 Requirements for Resistance to the Effects of Radiation

Orbiter avionics LRU's shall be designed and certified to meet performance and reliability requirements while operating within the ambient radiation environment of low earth orbits (LEO) at orbital inclinations of 28.5 to 90.0 degrees. The Orbiter vehicle must function within specification during exposure to trapped (Van Allen) radiation belts and solar plus galactic cosmic radiation. Orbiter radiation environment models and expected mission radiation levels are specified in Section 2.

Single event effects (SEE's) as well as total dose effects must be considered. The term single event effect is used here to include both single event upset (SEU) and latchup phenomena.

1.3.1 Single Event Upsets

Single event upsets are unintentional changes in the state of a bistable device induced by ionizing radiation. The LRU-level effect of any given SEU as well as the statistically predictable rate of occurrence must be considered to determine the necessity of internal architectural safeguards such as Error Correction Codes. Any SEU which propagates within the LRU so as to result in anomalous external performance (within the context of required Avionics Systems performance) is equivalent to a conventional failure mechanism, and therefore, must be accounted for in the derivation of Effective MTBF as defined in paragraph 1.4.1.

Latchup

Latchup of an electronics part is generally equivalent to failure of its host LRU. It is acknowledged that power cycling may occasionally restore proper operation; however, as is the case for SEU-induced anomalous LRU operation, the instantaneous effect on overall avionics systems performance would make even such a recovery scenario indistinguishable from conventional failure mechanisms. Thus, latchup susceptibility must be accounted for in the derivation of effective MTBF. For the purposes of defining latchup susceptibility, an electronic part which does not latchup when exposed to ions with a LET of 36 MeV cm²/mg or greater may be considered to have no practical latchup susceptibility.

Permanent damage [Blandford et. al. (1984)] of an electronic part, as a result of radiation induced breakdown of the gate oxide, is also equivalent to a failure of the host LRU. It is a nonrecoverable failure. However, the incorporation of devices susceptible to permanent damage will follow the same guidelines, for failure at the LRU level, as stated above for latchup.

Total Dose Effects

Total dose effects degrade the performance of microcircuits, modify chip timing, and may lead to degraded LRU performance or failure. Orbiter avionics shall be designed and certified to meet functional performance requirements after being exposed to the total dose specified in Section 2.1. If the use of the hardware or its planned lifetime is not consistent with the mission model described in Section 2.3, then an appropriate total dose requirement should be calculated and applied using the methodology described in Section 2.3.

1.4 Design Acceptance Criteria

The existing Orbiter avionics LRU's have demonstrated satisfactory immunity to single event effects in low and moderate inclinations in a nominal environment. The acceptance criteria for replacement designs is intended to perpetuate this satisfactory experience by maintaining as a minimum the current reliability of LRU's.

MTBF Definitions

The MTBF definitions herein are intended to provide a basis for comparing the anticipated performance of the new LRU with its predecessor. To simplify the procedure, only the contribution of electronic components will be considered without regard for other mechanisms such as solder joints or connectors. The computations at the LRU level should use standard handbook procedures such as Military Standard 756E (1981) and Military Handbook 217E (1986) (see Appendix C).

Reference MTBF The MTBF of the existing LRU should be calculated using the appropriate handbook values for component failure rates consistent with nominal operational thermal environments. This MTBF may be adjusted for the failure mechanisms discussed in paragraphs

1.3.1 and 1.3.2 if the existing LRU is susceptible to radiation effects. This value is considered as the Reference MTBF.

Effective MTBF The Effective MTBF for replacement hardware is computed with the same procedures as the Reference MTBF, except that the failure mechanisms discussed in paragraphs 1.3.1 and 1.3.2 must be considered. It is essential that the respective statistical component failure rates for SEE's be applied in a manner which accounts for any design features intended to preclude anomalous operation at the LRU level.

Please note that the conventional MTBF of replacement hardware will always show significant improvement over that of the original because of reduced component quantities inherent in newer technologies.

1.4.2 Acceptance Criteria

A design for an Orbiter avionics LRU is acceptable for resistance to radiation if the Effective MTBF is greater than the Reference MTBF, and the requirements regarding total dose (paragraph 1.3.3) are met.

1.5 Further Considerations

It is intended that the radiation environment will be considered in the design process to the extent necessary to preclude poor design decisions. The challenge is to design and certify to the radiation requirements with minimal cost and schedule impact.

The approach described in Section 1.4 allows the use of components with finite SEE rates if adequate architectural safeguards are incorporated to preclude propagation of the upset to the LRU level. Note that this does not sanction the use of latchup prone devices which, although protected, would still effectively disable the LRU.

Selection of electronic parts with adequate resistance to radiation effects is an integral step in the design process. Engineering judgment is required to screen parts lists and identify specific components whose function, quantity, and generic susceptibility warrant analysis or testing to provide the data necessary to support design decisions. When analysis and testing are warranted, the procedures described in Section 3 and Appendix A should be followed.

SECTION 2 RADIATION ENVIRONMENT

2. Natural Radiation Environment

The radiation environment the Orbiter will be exposed to is as follows:

- a) Single Event Effects. Two phenomena are responsible:
 - 1) direct deposition of charge on a critical node by the ionization of charged particles originating outside the spacecraft and
 - 2) ionization from the products of nuclear reactions caused by protons originating outside the spacecraft. For direct deposition single event rate calculations, the charged particle environment used herein consists of galactic and solar cosmic ray ions (hydrogen through uranium) and trapped (Van Allen) protons. For nuclear reactions caused by protons, the radiation environment consists of only the proton components of the above environment. These environments are defined in Section 2.2. The single event effect (upset and latchup) error rate produced in a given part by these environments is computed using the methods described in Appendix A.

- b) Total Dose. The environment is defined in Section 2.3. Section 2.3 gives the dose rate that parts will be exposed to and the total dose for one possible scenario of Orbiter lifetime usage. Based on this lifetime usage scenario, the total dose exposure design limit was established as the following:
 - 1) For parts located inside the Orbiter, there should be no system performance degradation as a result of exposure to a total dose of 1000 Rads (silicon)
 - 2) For parts outside the Orbiter, there should be no system performance degradation as a result of exposure to a total dose of 2000 Rads (silicon).

The dose rate data in Section 2.3 may also be used to compute total dose exposure for any given Orbiter lifetime usage scenario. For example, if extended duration Orbiter missions are planned, total dose exposure will be significantly greater than the values given in Table 2.3-2.

2.2 Single Event Effect Environment

2.2.1 Direct Deposition by Ions

The 90% worst-case environment defined by Adams (1986) was chosen to represent the typical cosmic ray space radiation that Orbiter avionics should be designed to withstand. To this, trapped (Van Allen) protons were added as described below.

The resulting "90% worst-case" radiation environment is to be used for direct deposition upset calculations and is defined by the integral LET spectra in Figures 2.2-1 and -2. The spectra are provided for a circular orbit altitude of 500 km for inclinations of 28.5, 57.0, and 90.0 degrees. The spectra are provided for two locations and were produced as follows:

- a) Two locations were chosen for definition of the radiation environment and will be referred to as the Internal location and the Free Space location:

Internal – A worst-case site internal to the Orbiter was determined to be the aft avionics Bay 4 at MDM FA-1. The environment for this location applies to all parts to be placed in the forward avionics Bay 1, 2, or 3 or the aft avionics Bay 4, 5, or 6. These Bays are defined in Hischke et. al. (1980). The Internal location is shown in Figure 2.2-3. The shield thickness for this location was calculated using the Elemental Volume Dose Program described in Hamilton and Liley (1976). The aluminum equivalent thickness of the Orbiter body was determined for 968 rays uniformly distributed in all directions emanating from this location. In addition to the shielding of the Orbiter itself, a 100 mil thick aluminum sphere was added. The resulting shielding for the Internal location is shown in Figure 2.2-4 which shows the distribution of rays versus thickness.

Free Space – The worst-case external location was chosen to be representative of free space shielded only by a 100 mil thick aluminum sphere. It applies to devices that may be placed sufficiently far from the Orbiter that shielding by the Orbiter is negligible. The environment for this location applies to the payload bay or outside the skin of the Orbiter. This location also applies to the OMS Pods and shelves near the payload bay. For the Free Space location, the shield thickness is 100 mils for every ray.

- b) The radiation environment was produced using the Cosmic Ray Effects on Microelectronics (CREME) code defined in Adams (1986) and references therein with the following input conditions:
 - 1) A quiet magnetosphere with no earth shadow was assumed for geomagnetic attenuation
 - 2) 90% Worst-case (M=3 CREME interplanetary weather index) galactic and solar cosmic rays at solar minimum transmitted through aluminum shielding described above
 - 3) fully ionized cosmic ray ions from hydrogen to uranium (z=1 to 92)
 - 4) Orbit averaged differential flux for trapped Protons computed using the National Space Science Data Center codes: ORP (Orbital Radiation Program) and ORB (Orbit Trajectory Generator Program). The AP8-MIN Vette model was used with a 1964 epoch and an International Geomagnetic Reference Field (IGRF) 1965 magnetic field. See for example: Curtis et. al. (1986) and Teague and Vette (1974). Trapped proton spectra are shown in Appendix D.

Figures 2.2-1 and -2 show that the 28.5 degree inclination orbit has significantly less radiation flux than the 57 and 90 degree orbits for both the Internal and the Free Space locations. This is due to the natural shielding provided by the earth's magnetosphere. Note also that the Free Space location flux is only about 2-5 times the Internal location flux for all three inclination orbits.

2.2.2 Nuclear Reactions Caused By Protons

The intensely ionizing particles that cause single event effects can be the fragments of a silicon nucleus struck by a particle originating outside the spacecraft. The most common particle in space capable of causing such a nuclear reaction is the proton. Therefore, the environment to be used in these calculations should consider cosmic ray and trapped (Van Allen) proton sources.

The proton environment used for proton upset calculations is defined by the differential energy spectra in Figure 2.2-5. These spectra were produced using the Cosmic Ray Effects on Microelectronics (CREME) code with the intentional omission of ions heavier than hydrogen. The following input conditions were used:

- 1) A quiet magnetosphere with no earth shadow was assumed for geomagnetic attenuation
- 2) 90% Worst-case (M=3 CREME interplanetary weather index) galactic and solar cosmic rays at solar minimum transmitted through 100 mil of aluminum shielding
- 3) cosmic ray hydrogen ions ($z=1$)
- 4) Orbit averaged differential flux for trapped Protons computed using the National Space Science Data Center codes: ORP (Orbital Radiation Program) and ORB (Orbit Trajectory Generator Program). The AP8-MIN Vette model was used with a 1964 epoch and an International Geomagnetic Reference Field (IGRF) 1965 magnetic field. See for example: Curtis et. al. (1986) and Teague and Vette (1974). Trapped proton spectra are shown in Appendix D.

These differential energy spectra should be used according to the procedures in Appendix A, to generate the upset error rates that result from nuclear reactions caused by protons.

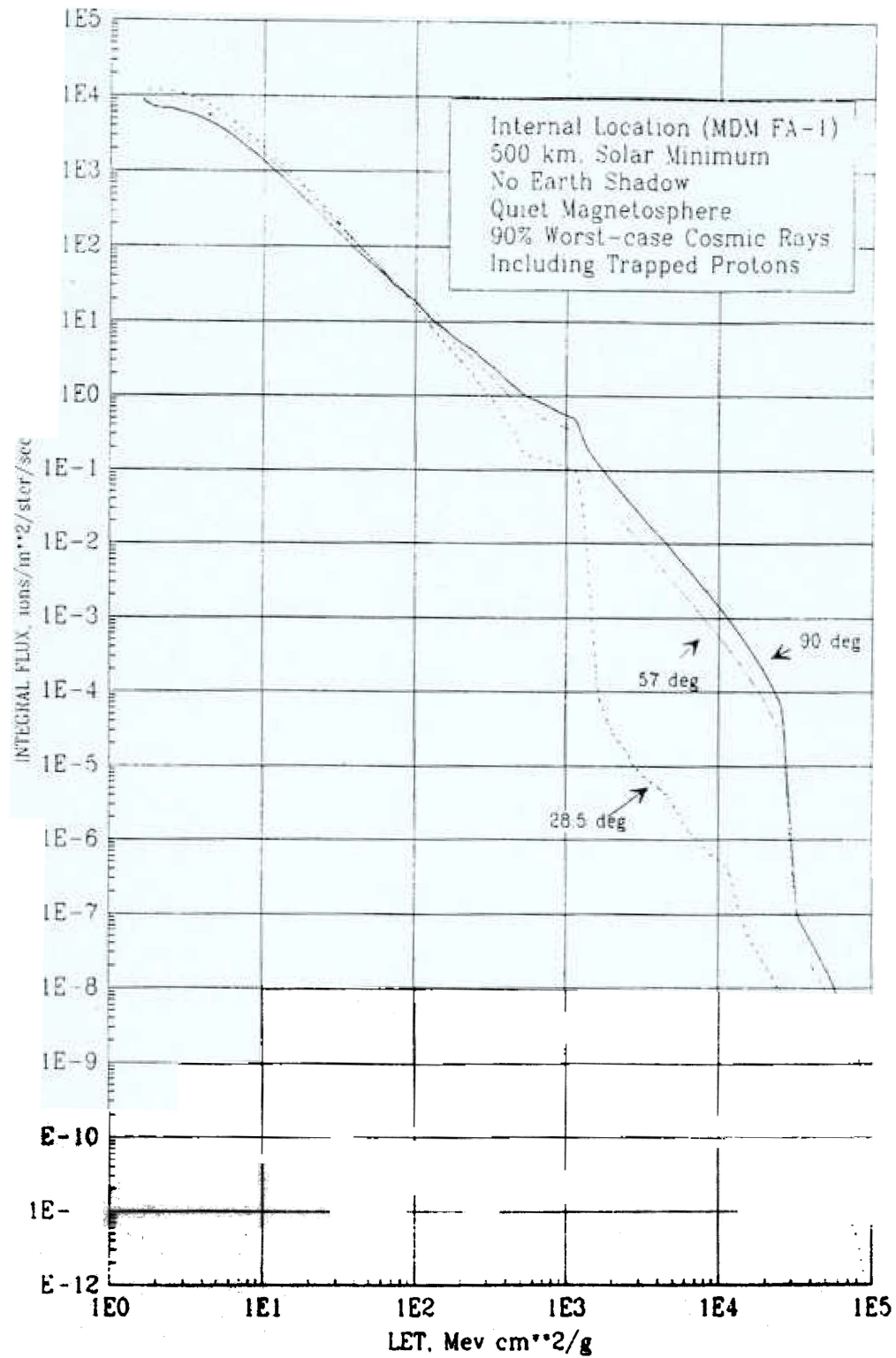


Figure 2.2-1 Integral LET (silicon) spectra for Internal location (MDM FA-1) for 90% worst-case (M=3, z=1 to 92) cosmic rays including trapped protons (AP8-MIN with 1965 IGRF magnetic field and 1964 epoch)

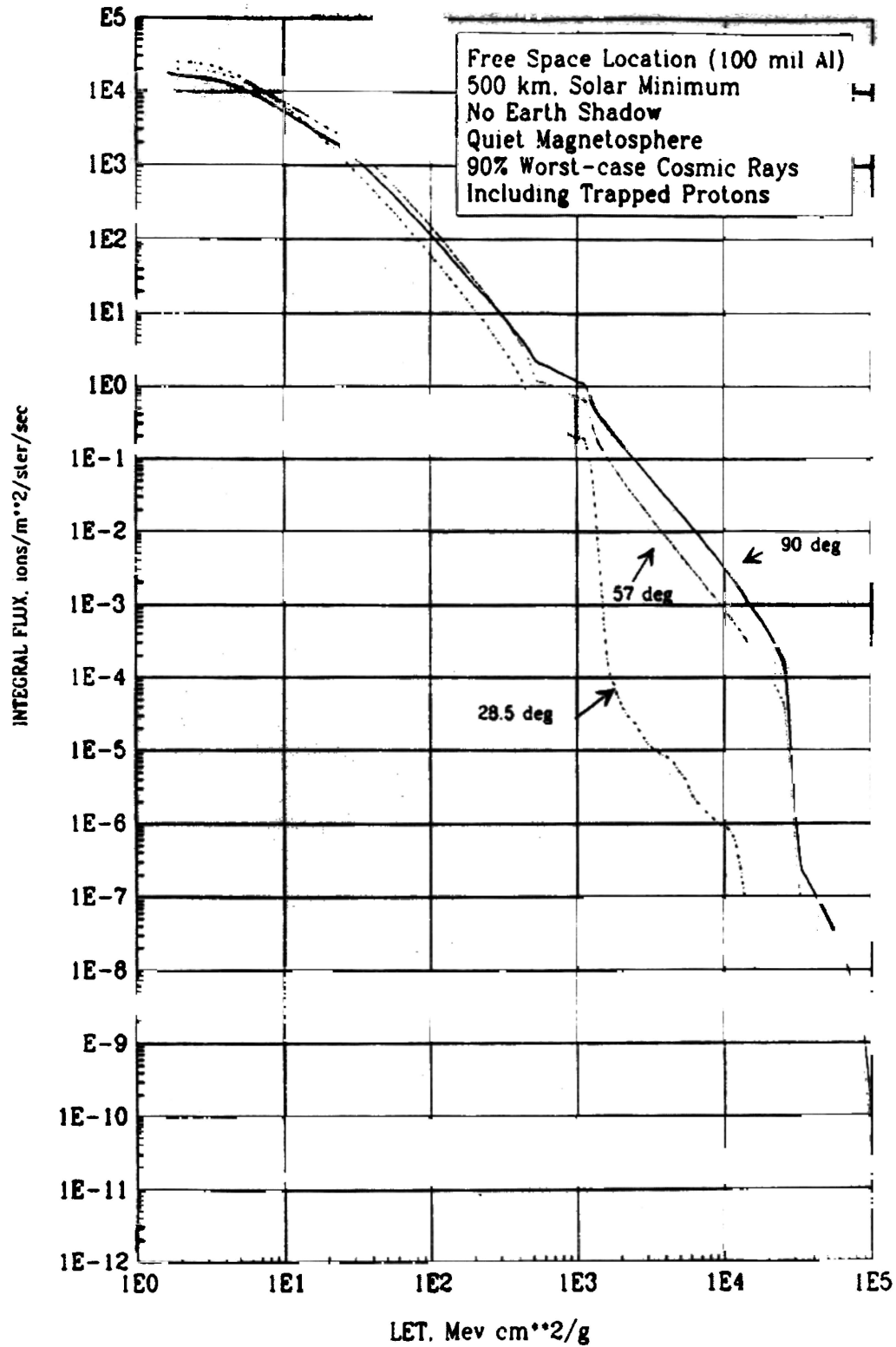
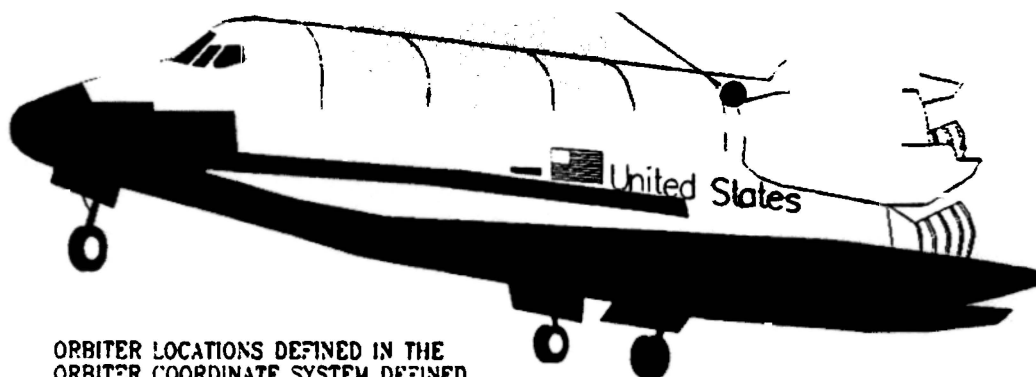


Figure 2.2-2 Integral LET (silicon) spectra for Free Space location (100 mil Al) for 90% worst-case (M=3, z=1 to 92) cosmic rays including trapped protons (AP8-MIN with 1965 IGRF magnetic field and 1964 epoch)

INTERNAL LOCATION*
MDM FA-01
X = 1323.35"
Y = -81.70"
Z = 394.80"



ORBITER LOCATIONS DEFINED IN THE
ORBITER COORDINATE SYSTEM DEFINED
IN HIRSCHKE ET. AL. (1980)

Figure 2.2-3 Orbiter location chosen for definition of internal radiation environment

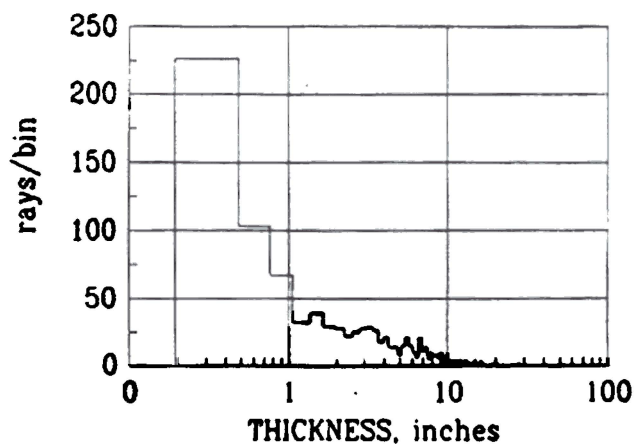


Figure 2.2-4 Ray distribution versus thickness of aluminum for
Internal Orbiter location (MDM FA-1)

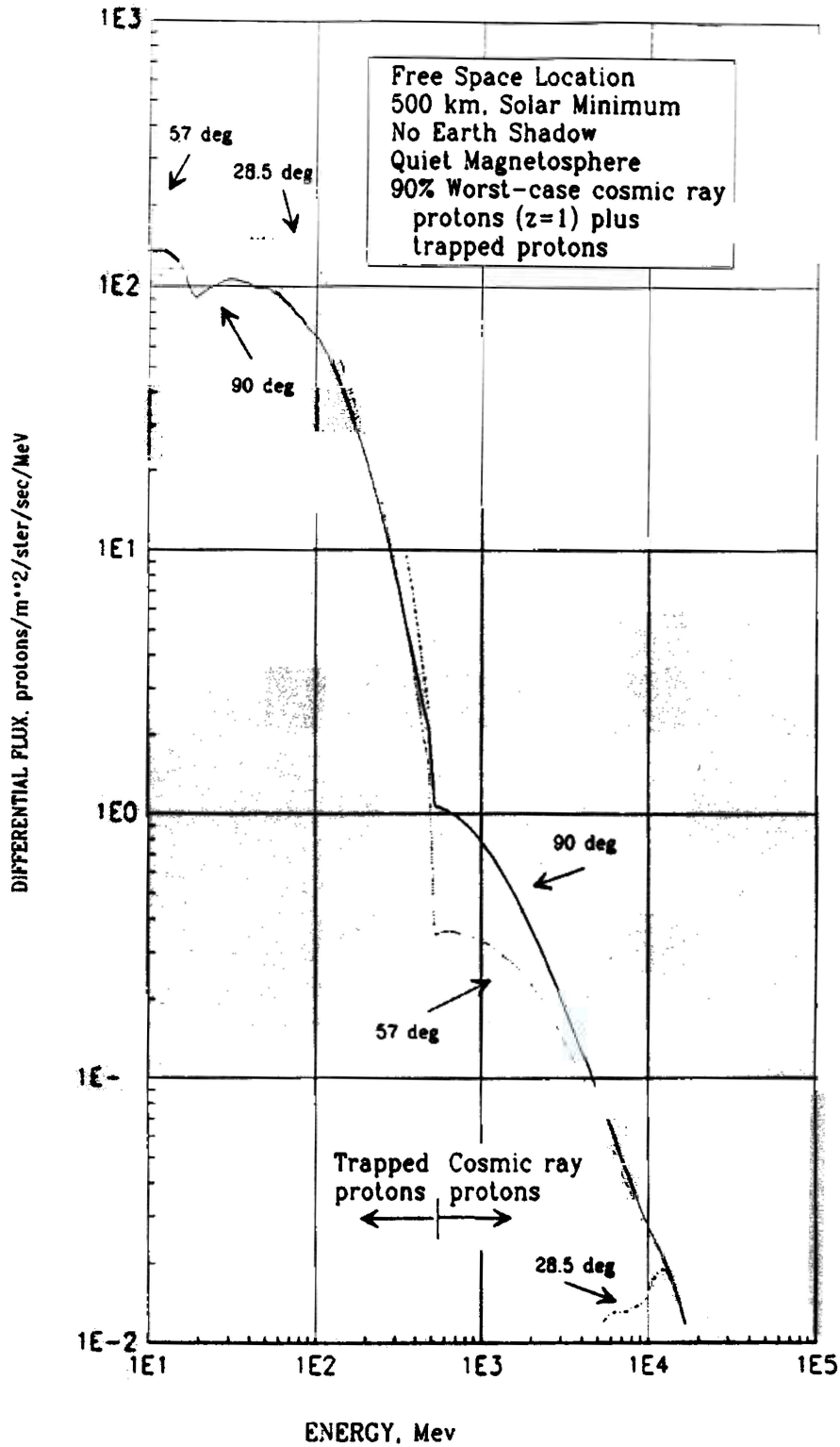


Figure 2.2-5 Differential energy spectra for Free Space location (100 mil Al) for 90% worst-case (M=3, z=1) cosmic ray protons including trapped protons (AP8-MIN with 1965 IGRF magnetic field and 1964 epoch)

2.3 Total Dose Effect Environment

The dose rates for the selected locations are shown in Table 2.3-1. These dose rates were determined assuming 90% worst-case radiation dose due to trapped protons and solar plus galactic cosmic rays as described in Section 2.2. In addition, the contribution of trapped electrons was also included since they produce bremsstrahlung radiation which contributes to part degradation. The trapped electron flux was determined similarly to the trapped proton flux as described in Section 2.2. Figure D.1-2 shows the resulting trapped electron spectra determined from the AE8-MIN model obtained by private communication with Vette.

LOCATION	DOSE RATE [rad (Si)/day]		
	28.5 deg	57.0 deg	90.0 deg
INTERNAL	0.150	0.110	0.100
FREE SPACE	0.400	0.540	0.460

Table 2.3-1 Dose rate for each location for each orbital inclination

The 90% worst-case dose rates in Table 2.3-1 were multiplied by the expected exposure time. This time was determined by assuming the following mission model:

- 500 km altitude
- 2) 80% of missions are at 28.5 degrees and 10% are at 57.0 and 90.0 degrees inclination
- 3) 5 days on-orbit per mission
- 4) 4 missions per year for each Orbiter
- 5) Orbiter lifetime of 20 years

In addition to the 90% worst-case total dose accumulated over the lifetime of each Orbiter, it was also assumed that each Orbiter would be exposed to one solar flare equal to the August 1972 solar proton event. Furthermore, the least geomagnetic shielding, that of a 90.0 degree inclination orbit, was assumed. The total radiation dose produced by the August 1972 solar proton event was generated using the free space expression for the proton fluence of King (1973):

$$J(\text{greater than } E) = 7.9 \times 10^9 e^{[(30-E)/26.5]}$$

The fluence J is in #/cm² and the energy is in MeV between 10 and 200 MeV and is plotted in Figure 2.3-1. This fluence was attenuated by the geomagnetic field for a 90.0 degree inclination and the aluminum shielding for the locations described above.

The total dose due to a lifetime exposure to the 90% worst-case environment plus exposure to one solar energetic particle event is shown in Table 2.3-2. A design margin of two (2) was applied to the total dose to arrive at the design limit for parts at each location. No allowance was made for annealing effects that might be experienced.

LOCATION		TOTAL DOSE [rad (Si)]
INTERNAL	90% WORST-CASE	60
	FLARE	90
	TOTAL	150
	DESIGN LIMIT (2X)	300
FREE SPACE	90% WORST-CASE	170
	FLARE	780
	TOTAL	950
	DESIGN LIMIT (2X)	1900

Table 2.3-2 Total dose exposure expected for Orbiter avionics at each location.

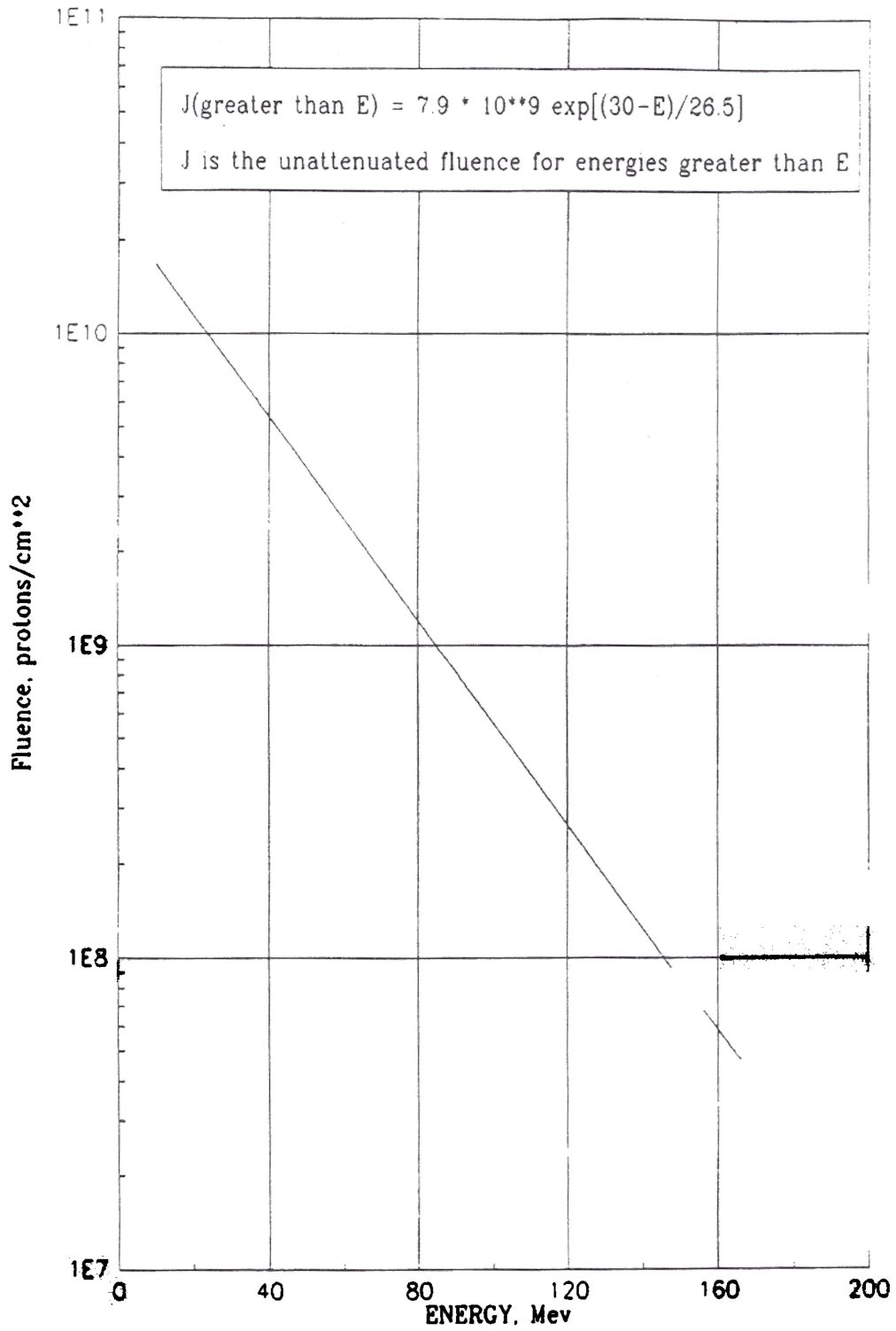


Figure 2.3-1 Total, integral proton fluence for August 1972 solar proton event according to King (1973)

2.4 Environment Error Analysis

The ability to predict the radiation flux as a function of LET or energy at a given location within the Orbiter depends on:

- 1) knowledge of the cosmic ray environment outside the magnetosphere
- 2) knowledge of the trapped (Van Allen) environment
- 3) prediction of solar energetic particle events radiation
- 4) attenuation due to the magnetosphere and the walls of the Orbiter
- 5) Orbiter vehicle attitude with respect to the sun and earth

The cosmic ray model developed by Adams (1986) is primarily based on measurements taken beyond the magnetosphere by numerous spacecraft and measurements made from stratospheric balloons. Adams estimates the model predicts the absolute cosmic ray flux within a factor of two where adequate data is available. This uncertainty arises primarily from the inability to predict future levels of solar modulation. The cosmic ray model contains a prediction for a 90% confidence level; i.e., the actual flux will exceed this level only 10% of the time. This is based on measurements of total fluence taken over six-hour intervals between 1973 and 1980. Therefore, the vehicle can expect to experience an environment modulation more severe than predicted 10% of the on-orbit time.

The trapped radiation model presented is based on the 1965 IGRF magnetic field used with a 1964 epoch (flux data). However, it is well known that the magnetic field is decreasing in magnitude and drifting westerly. This approach (1965 field, 1964 epoch) was chosen because it predicts a constant trapped radiation environment over the years and this is supported by dosimeters flown on recent STS missions according to Atwell (1987).

For single event effects, the 90% worst-case environment is recommended for design calculations. However, for total dose design calculations, the August 4, 1972 solar flare was considered as a representative worst-case solar flare. This was a large flare which produced a fluence at earth nearly twice the sum of all the other flares in this active period. There is no guarantee that a flare of this magnitude will occur over the life of the Orbiter. However, since most active periods display one anomalously large event, its consideration cannot be neglected.

Figure 2.4-1 and -2 show the solar energetic particle environment defined by Adams (1986) as the "peak Aug. 4, 1972 flare flux and mean composition." It should be noted that for the 28.5 degree inclination orbit, the LET spectra for the flare is about the same as for the 90% worst-case. Figure 2.4-2 does not contain trapped protons and is provided to show that trapped protons have little effect on the 57 and 90 degree orbits for flare conditions.

Errors introduced into particle flux predictions by attenuation by the magnetosphere and the Orbiter walls are small. Uncertainties in the geomagnetic cutoff and earth shadowing attenuation predictions translate into no more than a +/-30% error in particle flux according to Adams (1981). The wall attenuation calculation neglects projectile fragments. This leads to a systematic underestimate of particle fluxes. However, this error is negligible for wall thicknesses less than 50 g/cm² [7.3 inches (Al)]. Figure 2.2-4 shows that very few of the rays from the Internal Orbiter location are greater than 7.3 inches (Al).

Orbiter vehicle attitude effects were not modeled for several reasons: the cosmic ray and trapped proton models provide isotropic fluxes of particles, the vehicle attitude is mission dependent, and each Orbiter location has a unique directional radiation susceptibility due to shielding. However, these calculations are conservative because the Internal and Free Space locations were chosen such that they are the worst-case of all internal and external locations. That is, the 100 mil Al sphere in free space is more exposed than any 100 mil Al sphere placed in the payload bay or anywhere outside the Orbiter.

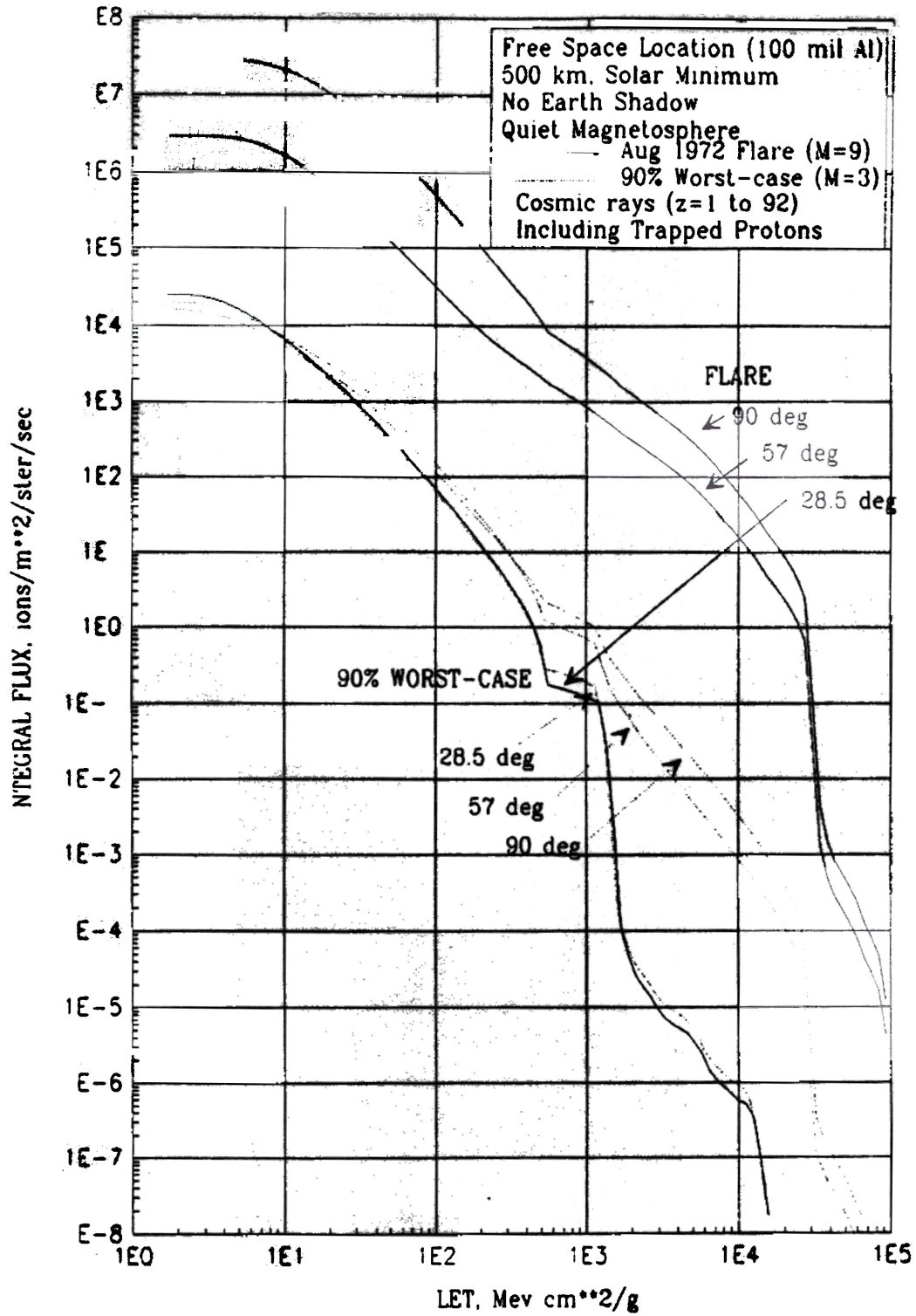


Figure 2.4-1 Integral LET (silicon) spectra for Free Space location (100 mil Al) for August 1972 solar flare (M=9, z=1 to 92) and 90% worst-case (M=3, z=1 to 92) cosmic rays including trapped protons (AP8-MIN with 1965 IGRF magnetic field and 1964 epoch)

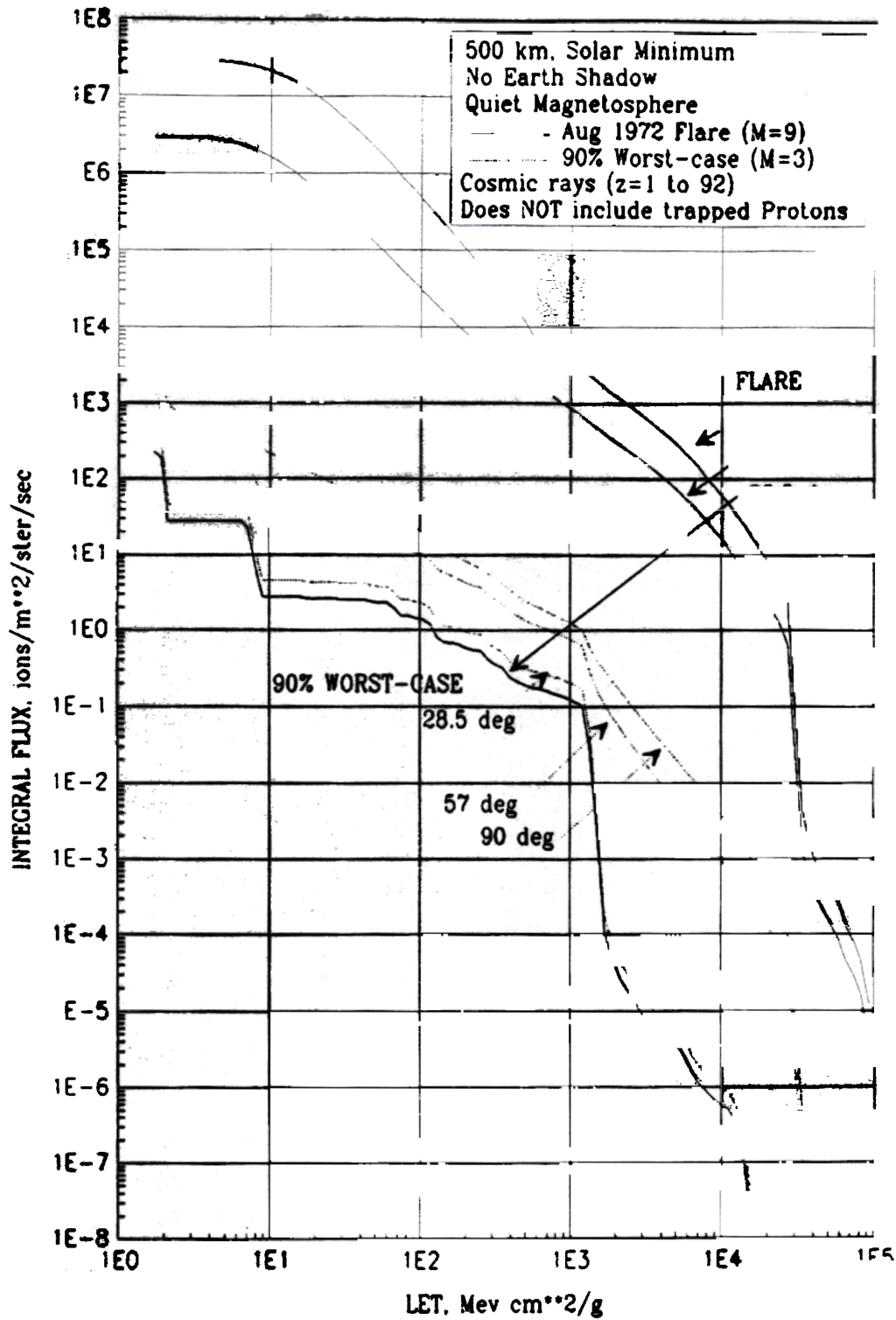


Figure 2.4-2 Integral LET (silicon) spectra for Free Space location (100 mil Al) for August 1972 solar flare (M=9, z=1 to 92) and 90% worst-case (M=3, z=1 to 92) cosmic rays without including trapped (Van Allen) protons

SECTION 3

QUALIFICATION OF ELECTRONIC COMPONENTS AND SYSTEMS

3.1 Introduction

Qualification of electronic components and systems should always be based on radiation testing of the components and systems. The degree of testing and analysis necessary to qualify a component for a new design or an existing, complete system of components varies considerably. The system application criticality and the degree of risk the program is willing to accept for a given application operating in a given radiation environment determines which tests must be performed. In principle, the ionizing radiation spectrum used for testing should be comparable to that of the system application environment. Since this is possible only for the most benign applications, the best that can be done is to evaluate the degree of risk remaining based on the level of testing performed and the program can decide if this is acceptable.

The following paragraphs describe ionizing radiation testing methods that may be used. These tests include 1) low energy heavy ion testing, 2) high energy proton testing, and 3) high energy heavy ion testing. Each test is capable of emulating a different portion of the natural space ionizing radiation spectrum and each has its own realm of practicality since test cost and complexity vary enormously. Low energy heavy ion testing is generally used to qualify individual components for new designs. High energy proton and/or heavy ion testing is an effective way to qualify existing, complete system of components as well as new designs.

3.2 Single Event Effect Testing Of Electronic Components

3.2.1 Low Energy Heavy Ion Testing

For new system designs, low energy heavy ion testing (or use of existing test data) may be warranted. This approach exposes individual components of the system to low energy (typically around 12 MeV/nucleon) heavy ions at LET's up to 60 - 100 MeV cm²/mg. The range of these ions is so small that the components or device under test (DUT) must be de-lidded and operated in a vacuum chamber. During exposure, the DUT must be adequately monitored for Single Event Effects (SEE's). Exposure to 10⁶ ions/cm² virtually guarantees that all SEE's that could occur in low earth orbit will be detected. For SEE's observed, on-orbit SEE rates can be calculated for both the heavy ion and proton environments defined in this handbook. These methods are described in (Connell, 1995) for heavy ion environments and in (Rollins, 1990) for proton environments.

Facilities such as the Tandem Van de Graaff Accelerator Facility at the Brookhaven National Laboratory, the 88" cyclotron at the Lawrence Berkeley Laboratory, or the K-500 cyclotron at Texas A & M are available for low energy heavy ion testing.

3.2.2 High Energy Proton Testing

High energy (200 MeV or greater) proton testing of microelectronic components, whether individually or in complete systems, is a practical, reliable method for determining SEE and Total Ionizing Dose (TID) susceptibility (Foster, 1996 and 1997). Proton tests are normally performed with the DUT operating in air - as opposed to a vacuum chamber. The DUT is exposed to a high energy beam of uniform cross section (typically about 7 cm in diameter).

The high proton beam energy of 200 MeV is sufficient to pass completely through the DUT which has a thickness equivalent to 3.3 inches of aluminum (22.7 g/cm² mass thickness). For this thickness, the beam does not lose more than 50% of its energy by passing through the DUT. Many complete systems are packaged such that this thickness is not exceeded and thus avail themselves of high energy proton testing. Obviously, components do not need to be de-lidded and they are tested at their normal operating temperature.

The ionizing radiation environment produced by the 200 MeV proton beam within the sensitive regions of microelectronic components is comparable to several earth orbit environments. The best concurrence is with the proton spectra experienced in earth orbits that pass through the South Atlantic Anomaly and during periods when protons from solar flares penetrate the earth's magnetosphere. These spectra have energies comparable to proton test energy (200 MeV) and there are satisfactory methods (Bendel, 1983) for predicting on-orbit SEE rates for these environments based on the SEE rates observed during proton testing.

In addition, the on-orbit SEE rate for earth orbit heavy ion environments based on high energy proton test SEE rates can be predicted. The analytical model (O'Neill, 1998) indicates that the LET spectra produced in components by protons during testing extends up to about 14 MeV cm²/mg. Therefore, many of the failure modes caused by heavy ions in space will be detected in high energy proton testing. Using the analytical model (O'Neill, 1998), the LET spectrum produced in the sensitive volumes of components by 200 MeV protons is compared to the natural space environment due to heavy ions for various earth orbits. The result is that a proton test exposure of 10¹⁰ protons/cm² is equivalent to various number of years exposure on-orbit to heavy ions. According to (O'Neill, 1998) an *upper bound* on-orbit SEE rate for a typical medium inclination orbit (55 degrees/270 nmi/solar minimum/0.1" aluminum) is found by assuming that 2 years on-orbit is equivalent to a proton test exposure of 10¹⁰ protons/cm². According to (Petersen, 1998) a *good estimate* on-orbit SEE rate for a typical medium inclination orbit (55 degrees/270 nmi/solar minimum/0.1" aluminum) is found by assuming that 6 years on-orbit is equivalent to a proton test exposure of 10¹⁰ protons/cm².

Also, the high energy proton test results can be used to determine the risk of experiencing a failure (such as a latch-up or burn-out) in a heavy ion environment that was not observed during the proton test. The number of these failures observed during high energy proton testing depends on the LET threshold and the cross section of the failure mode. Increasing the magnitude of the cross section increases the chance of observing a given failure while it also increases the on-orbit SEE rate for that failure. Similarly, decreasing the threshold LET has the same effect. This allows the probability that a given failure will be experienced during a typical 200 MeV proton test exposure (10¹⁰ protons/cm²) as a function of the on-orbit Mean-Time-Between-Failures (MTBF) to be determined (O'Neill, 1998). Here, the concern is not with prediction of upset rate in space based on observed upsets during proton testing, but about the failures that were not

observed during proton testing. In other words, if a part is tested with protons (say at 200 MeV) and no failures (such as latch-up) are observed, what can be said about the parts performance (i.e. without latch-up) in a heavy ion environment such as that found in earth orbit? According to (O'Neill, 1998), there is a very high (nearly 1.0) probability that all failures possible with MTBF less than 10 - 100 years will be caught during proton testing.

However, some devices with larger feature sizes will not actually latch-up with high energy protons as often as the model predicts. Based on actual observations, the minimum MTBF guaranteed is about 10 years.

Therefore, following proton testing, the program manager has the following information about SEE susceptibility for the device tested. He knows the SEE rate in the proton and in the heavy ion environment for the failures he did observe. He also knows that the MTBF is at least about 10 years for the "harder" failures in the heavy ion environment that he did not observe. He can then decide if the device tested is acceptable for the planned application.

If the on-orbit SEE rate predicted based on the observed failure modes is acceptable for the proton and heavy ion components of the environment and an MTBF of 10 years for hard failures is acceptable, the system is accepted. Otherwise, high energy heavy ion testing must also be performed.

Facilities such as the Indiana University Cyclotron Facility produce protons up to 200 MeV and are available for high energy proton testing.

3.2.3 High Energy Heavy Ion Testing

High energy heavy ion testing can be used for both component level testing and system level testing. For certain mission critical applications, high energy heavy ion testing may be used to obtain a higher degree of radiation hardness assurance than obtained from high energy proton alone. This is normally found by also testing with heavy ions at higher LET's than can be produced by 200 MeV protons.

In cases where the application warrants it (cost of system, safety, criticality), heavy ion testing is desirable in addition to proton testing. Facilities such as the Alternate Gradient Synchrotron (AGS) at the Brookhaven National Laboratory provide beam energies of 10 GeV/nucleon gold ions which produce an LET of 12 MeV cm²/mg at normal incidence. The range of these ions is much greater than that of the recoil ions produced by 200 MeV protons and is sufficient to latch-up any device with a measurable cross-section below an LET of 12 MeV cm²/mg. For devices that require ions with range on the order of 35 - 40 μ to induce latch-up, this testing can significantly increase the radiation hardness assurance determined using 200 MeV proton testing.

Also, the National Super-conducting Cyclotron Laboratory at Michigan State University has recently become available. This facility can produce 80 MeV/nucleon heavy ions which can penetrate devices without de-lidding. This facility might also be used for system level testing to further reduce the on-orbit risk for the more critical systems.

3.3 Total Dose Testing

For all practical purposes, total dose testing for Orbiter and GFE components is un-necessary. The Orbiter lifetime dose is small (less than 1000 rad(silicon)) for any devices shielded by a few hundred mil aluminum or more. Total dose testing could be warranted only for the rare device(s) that have minimal total shielding. In these rare cases, dose analysis should be done to determine whether or not total dose testing is necessary.

3.4 Conclusion

In order to insure the most efficient and minimal risk system development and/or system procurement, each system application must be analyzed according to the following:

- is the system being built from selected devices (e.g. new Shuttle flight computers, space station communication system, etc.)?
- is the system being purchased as a complete avionics package containing many devices (e.g. Laptop computers, Inertial Navigation System - Global Position System, etc.)?
- what is the system's flight criticality, is safety affected?
- what is the radiation environment (orbit, shielding, etc.)?

For many new space applications, there is no hope of performing low energy heavy ion testing on any, let alone all of the devices in the system. There are hundreds of devices and many are plastic encapsulated and some do not have part identification (so even similarity analysis can not be done). In these cases, testing at the system level is the only option - aside from no testing at all before it is put in space. For these systems high energy proton and/or heavy ion testing makes sense. It identifies practically all the failures that can happen on a frequent basis (MTBF of 10 years or less). It is relatively inexpensive and can be done on short notice with minimum preparation of test fixtures. Also, system level proton and/or heavy ion testing screens all of the devices in the system. Few systems are built with 100% knowledge of their heavy ion cross-sections. Often, devices are accepted based on "similarity analysis". This is very risky, it is too easy for a component manufacturer to modify his line and change a "hard" chip into one with a very "soft" latch-up/burn-up problem.

High energy proton and/or heavy ion testing is also applicable for systems being developed from new components. Quite often, even these systems contain too many components and their application is not critical enough to warrant low energy heavy ion testing of every chip in the box. System designers should not be forced to use only tested, radiation hard parts. A much more robust design can usually be obtained using state-of-the-art commercial devices that don't have a radiation pedigree. Most of these devices are acceptable for the low earth orbit environment and high energy proton and/or heavy ion testing can efficiently identify the devices that aren't. Selected use of these chips can help make systems run faster, perform better, and cost less.

REFERENCES

- Adams Jr., J.H., R. Silberberg and C.H. Tsao, "Cosmic Ray Effects on Microelectronics, Part I: The Near-Earth Particle Environment," Naval Research Laboratory Memorandum Report 4506, August 25, 1981. (AD-A103897)
- Adams Jr., J.H., "The Variability of Single Event Upset Rates in the Natural Environment," IEEE Trans. on Nucl. Sci., Vol. NS-30, 4475-4480, 1983.
- Adams Jr., J.H., "Cosmic Ray Effects on Microelectronics, Part IV," Naval Research Laboratory Memorandum Report 5901, December 31, 1986.
- Adams Jr., J.H., Private communication, 1987.
- Adams Jr., J.H., "An Upper Limit on SEU Rates", Presented at the Orbiter Avionics Radiation Working Group Meeting No. 4, June 1988.
- Atwell, W., E.R. Beever, and A. Hardy, "Radiation Shielding Analysis for the Space Shuttle Program: An Overview," Presented at the Nuclear Society Topical Conference on Theory and Practices in Radiation Protection and Shielding, Knoxville, TN, April 22-24, 1987.
- Bendel, W.L., and Petersen, E. L., "Proton Upsets in Orbit," IEEE Transactions on Nuclear Science, Vol. NS-30, No.6, December 1983.
- Blandford, Jr., J.T., A.E. Waskiewicz, and J.C. Pickel, "Cosmic Ray Induced Permanent Damage in MNOS EAROMs," IEEE Transactions on Nuclear Science, Vol. NS-31, No. 6, December 1984.
- Chlouber D., "Upper Bound on Single Event Upset Rate," presented at the Orbiter Radiation Specification Working Group Meeting No. 4, June 1988.
- Connell, L. W., F. W. Sexton, A. K. Prinja, " Further Development of the Heavy Ion Cross Section for Single Event Upset: Model (HICUP)," IEEE Transaction on Nuclear Science, NS-42, 2026, December 1995.
- Curtis, S.B., W. Atwell, R. Beever and A. Hardy, "Radiation Environments and Absorbed Dose Estimations on Manned Space Missions," Adv. Space Res., Vol. 6, No. 11, pp 269-274, 1986.
- Foster, C. C., S.L. Casey, A.L. Johnson, P. Miesle, N. Sifri, A.H. Skees, and K. M. Murray, "Opportunities for Single Event and Other Radiation Effects Testing and Research at the Indiana University Cyclotron Facility," IEEE Nuclear Science and Radiation Effects Conference Workshop Proc., (July 1996).
- Foster, C. C., S.L. Casey, A.L. Johnson, P. Miesle, N. Sifri, A.H. Skees, and K. M. Murray, "Radiation Effects Test Facility at the Indiana University Cyclotron Facility," 14th International Conference on the Application of Accelerators in Research and Industry Workshop Proc. held in

Denton, Texas (April 1997).

Guenzer, C.S., E.A. Wolicki, and R.G. Allas, "Single Event Upset of Dynamic RAMs by Neutrons and Protons," IEEE Transactions on Nuclear Science, Vol. NS-26, No. 6, December 1979.

Hamilton, S.C. and B. Liley, Rockwell International Document No. SD 76-SA-0184-1, 1976

Hischke, E.R., W.J. Gaylor and M.A. Collins, "Shuttle Operational Data Book," NASA JSC 08934, Vol. 2, Rev. B, p 2.1-1, August 1980.

King, Joseph H., "Solar Proton Fluences as Observed During 1966-1972 and as Predicted for 1977-1983 Space Missions," NASA Goddard Space Flight Center Report X-601-73-324, 1973. See also, J.H. King, J. Spacecraft and Rockets, Vol.11, No.6, 1974.

Kolasinski, W.A., J. Elder, R. Koga, and J. Osborn, "On Heavy Ion Induced Multiple Upsets in Static and Dynamic Rams," Sixth Annual Symposium on Single Event Effects, April 1988.

Konradi, Andrei, Alva C. Hardy and William Atwell, "Radiation Environment Models and the Atmospheric Cutoff," Journal of Spacecraft and Rockets, Vol. 24, No. 3, pp 284-285, May-June 1987.

Messenger, George C., "Collection of Charge on Junction Nodes from Ion Tracks," IEEE Transactions on Nuclear Science, Vol. NS-29, No. 6, December 1982.

"Military Standard Reliability Modeling and Prediction," MIL-STD-756B, 18 November 1981

O'Neill, P.M., G.D. Badhwar, W.X. Culpepper, "Internuclear Cascade - Evaporation Model for LET Spectra of 200 MeV Protons Used for Parts Testing," IEEE Transaction on Nuclear Science, Vol 45, No 6, 2467, December 1998.

Petersen, E. L., J.B. Langworthy, and S.E. Diehl, "Suggested Single Event Upset Figure of Merit," IEEE Transactions on Nuclear Science, Vol. NS-30, 1983.

Petersen, E. L., "Soft Errors Due to Protons in the Radiation Belt," IEEE Transactions on Nuclear Science, Vol. NS-28, No. 6, December 1981.

Petersen, E. L. "The SEU Figure of Merit and Proton Upset Rate Calculations," IEEE Trans Nuc. Sci., Vol. 45, No. 6, 2550, December 1998.

Pickel, James C. and James T. Blandford Jr., "Cosmic-Ray-Induced Errors in MOS Devices," IEEE Trans. on Nucl. Sci., Vol. NS-27, 1006-1015, 1980.

"Reliability Prediction of Electronic Equipment", MIL-HDBK-217E, 27 October 1986.

Rollins, J.G., "Estimation of Proton Upset Rates from Heavy Ion Test Data," IEEE Trans. Nuc

Sci. NS-37, 1961, 1990.

Teague, Michael J. and James I. Vette, "A Model of the Trapped Electron Population for Solar Minimum," National Space Science Data Center, NASA/GSFC, Greenbelt, MD, Rept. NSSDC 74-03, April 1974.

Zoutendyk, J. A., "Modeling of Single-Event Upset in Bipolar Integrated Circuits," IEEE Trans. on Nucl. Sci., Vol. NS-30, 4540-5, 1983.

Zoutendyk, J.A., C.J. Malone, and L.S. Smith, "Experimental Determination of Single Event Upset as a Function of Collected Charge in Bipolar Integrated Circuits," IEEE Trans. on Nucl. Sci., Vol NS-31, 1167-1174, December 1984.

APPENDIX A

SINGLE EVENT RATE COMPUTATIONS

A high energy ion passing through a semiconductor creates an ionization trail of electron-hole pairs along its path through the material. A single event upset (SEU) occurs when a sufficient amount of energy is deposited so that enough charge is collected on one of the sensitive storage nodes of the chip to cause the binary state of the device to change. A latchup occurs when a parasitic silicon controlled rectifier is created within the device.

The purpose of this section is to outline the method of predicting the rate at which SEE's occur using the known high energy particle environment and device parameters. We follow the method given in the CREME IV report Adams (1986) to define the quantities characterizing the orbital environment and semiconducting devices and then compute the rate at which ionization induced errors in the circuit are expected to occur in the given high energy particle environment.

A Background Theory

A.1.1 Charged Particle Environment

The particle flux $F(E)$ [in units of particles/(m² ster sec)] is a function of the kinetic energy (E) per mass number (u) and is used to define the differential energy spectrum (dF/dE) of the particles. Since the spatial rate of energy deposition or LET (L) in a material is the important physical quantity determining whether an upset will occur, the differential energy spectrum is transformed to a differential LET spectrum according to

$$dF/dL = dF/dE * (dL/dE) \quad (A-1)$$

The LET energy dependence, defining the transformation factor dL/dE , is given for a variety of ions incident on silicon in Figure A.1-1 reproduced from Adams (1986). Examples of differential energy and LET spectra are given in Sections A.5 and 2.2 respectively. In contrast to linear energy transfer is stopping power, which is the rate at which an incident ionizing particle loses energy per unit pathlength. The stopping power of an ion is not necessarily the same as the LET. For an example, when high energy ions are incident on a target creating secondary electrons, which are sufficiently energetic to escape from the target material, the electrons carry away a portion of the energy lost by the incident particle. In this case the stopping power in the target is the sum of the LET plus the energy carried away by the escaping electrons.

Adams (1983) gives comparison calculations of cosmic ray spectra behind various amounts of shielding for cases in which the transport calculation includes contributions to LET from fragments of the incident cosmic rays that were broken up in collisions with nuclei in the spacecraft and the case where contributions from fragments are neglected. His results show that the distinction between these two cases only becomes important for cosmic rays passing through

large amounts of shielding (more than 7 inches of aluminum). Therefore, in this document we will use the simpler transport calculation that does not include contributions from fragments.

Because of the singularities in slope occurring in the differential LET spectra, the integral LET spectrum representation of the data is preferred. It is defined by

$$F(L_o) = \int_{L_o}^{L_{\max}} dF / dL dL \quad (\text{A-2})$$

$F(L_o)$ represents the flux of ions having a LET(L) such that $L_{\max} \geq L \geq L_o$. If L_o is taken to be the minimum LET required to induce an upset in the circuit, then the flux of particles with LET greater than L_o is a measure of the upset rate to be expected. Thus for various amounts of shielding, the integral LET spectra may be compared directly to determine the relative upset rates. Figure 2.2-2 shows some typical integral LET spectra for the Free Space location at 500 km altitude. Comparing Figures 2.2-2 and A.1-1, it can be seen that there is a correlation between the ledges in Figure 2.2-2 and the peak LET for iron (28 MeV cm²/mg), helium (1.6 MeV cm²/mg), and hydrogen (0.5 MeV cm²/mg) in Figure A.1-1. This is related to the sharp drop in elemental abundances just above iron, helium, and hydrogen.

A.1.2 Device Characteristics for Bit Errors

The energy deposited (E_{dep}) in the material by the ionizing particle depends linearly on the LET(L) and the length of the track(s) through the sensitive region of the semiconducting microcircuit

$$E_{\text{dep}} = L * s \quad (\text{A-3})$$

wherein L has units of millions of electron volts (MeV) per centimeter, s is in centimeters and E_{dep} has units of MeV. The track length(s) is measured in centimeters; however, in the literature shielding thickness is often expressed in g/cm² according to the definition

$$s(\text{g/cm}^2) = \text{density}(\text{g/cm}^3) * s(\text{cm}) \quad (\text{A-4})$$

In this case LET would be measured in units of MeV cm²/g.

The charge in picocoulombs(pC), created along the ionizing particle's path, due to the production of electron hole pairs at a rate of one pair for each 3.6 electron Volts(eV) of deposited energy, is given by

$$Q_{\text{dep}} = E_{\text{dep}} / (22.5 \text{ MeV per pC}) \quad (\text{A-5})$$

One way that an upset can occur at the site of an active junction is: The incident particle creates free electrons and holes in the junction and the depletion region under it. Electron-hole pairs in the depletion region are separated by the high electric field and collected on the junction, helping to neutralize the charge on the node which distinguishes the binary "off" state from the "on." Whenever the charge (Q_{dep}) is greater than a critical charge (Q_c), the logic state of the memory register is changed and an upset has occurred. In terms of the LET of the incident ionizing particle, a bit error occurs whenever the LET exceeds a critical value L_c for the pathlength(s)

$$L \geq 22.5 \text{ MeV per pC} * Q_c/s = L_c(s)$$

The absolute minimum LET (L_o), required to trigger an upset, occurs for the maximum pathlength through the sensitive region and is given by:

$$L_o = L_c(s_{max}) \quad (\text{A-7})$$

A.1.3 Single Event Upset Rate Formulation

The error rate is equal to the number of particles per unit time which deposit an amount of energy in the sensitive region in excess of the critical value

$$E_c = 22.5 \text{ MeV per pC} * Q_c$$

In terms of the LET spectrum, this occurs whenever

$$L_c(s) \geq L_o \quad (\text{A-9})$$

Consequently the upset rate depends only on the integral LET spectrum and the distribution of possible pathlengths within the sensitive region of the part. As given in Pickel and Blandford (1980), the upset rate (upsets/bit/sec) is given by

$$U_R = 4\pi A_p * \int_{s_{min}}^{\infty} F[L_c(s)] * C(s) ds \quad (\text{A-10})$$

wherein A_p is the mean projected area and $C(s)$ is the pathlength distribution, which is determined by the dimensions of the sensitive volume which is assumed to be a rectangular parallelepiped. The lower integration limit is the minimum pathlength for which stopping ions with maximum LET can deliver the critical charge

$$s_{min} = 22.5 \text{ MeV per pC} * Q_c/L_{max} \quad (\text{A-11})$$

In summary, given the ionizing particle environment (defined by the integral LET spectrum) and the device parameters for critical charge and dimensions of the sensitive volume, the single event upset rate is determined using equation (A-10). Experimentally only the threshold LET and the cross sectional area of the part perpendicular to the plane of the chip are known. The length to width ratio (aspect ratio) and the depth of the sensitive region are in general unknown from the experiments contemplated. They can, however, be estimated from manufacturers data if available. The method for determining the part parameters is given in section A.4.

A.1.4 Experimental Threshold LET

It is assumed that a cell's sensitive regions are represented by a slab of length(*l*), width(*w*), and height(*h*). An accelerator provides a source of ions of known energy or equivalent LET. Following the method outlined in Pickel and Blandford (1980), the threshold LET is determined as follows:

Accelerator ions are presumed to impact the surface of the part at an angle of incidence(*i*) as illustrated in Figure A.1-2. To vary the amount of energy deposited in the sensitive volume, we can change the energy of the ions coming from the accelerator or the angle of incidence of the ions onto the plane of the chip. Varying the angle of incidence(*i*) varies the pathlength [$s = h/\cos(i)$] and consequently the total energy deposited. Assuming that the ions pass entirely through the sensitive region and that the LET(*L*) does not change significantly along the path, the amount of energy deposited is given by equation (A-3). If we define the effective LET by [$L_{eff} = L/\cos(i)$], it can be seen that varying the angle of incidence of the ions allows us to effectively change the LET of the ions without changing the energy of the incident beam. At the Brookhaven Tandem Van de Graaff accelerator, for example, it takes 10-20 minutes for an energy change; therefore, changing the angle of incidence provides an efficient technique for small LET changes.

The method used is to vary the effective LET of the ions until the LET threshold(L_{th}), at which upsets just begin to occur, is identified. This corresponds to deposition of a critical amount of energy in the sensitive regions of the part. Using equations (A-3) and (A-8), the corresponding critical charge in picocoulombs associated with each bit error is given by

$$Q_c = L_{th} * h / (22.5 \text{ MeV per pC}) \quad \text{A. 2)}$$

If it is desired to compute the actual upset rate, the critical charge can be determined by experimental or analytical methods; for example, if sufficient device parameter data are available, the SPICE circuit analysis code [see Zoutendyk (1983)] can be used to analytically inject charges at sensitive junctions until the critical amount of charge to trigger an upset is determined. Alternatively, the critical charge can be determined experimentally as described in Zoutendyk (1984). If an experiment is then performed to determine the threshold LET, the effective depth of the sensitive volume can also be computed.

A.5 Dimensions of the Sensitive Region

The dimensions of the region sensitive to the incident particle ionization are estimated using manufacturers' data and the experimental upset cross section information obtained from accelerator tests.

As described in Pickel and Blandford (1980), the effective area of the sensitive region in the plane of the part may be determined from experimental cross section data, for example, if binary zeros are first stored in the bit registers and the part is subsequently irradiated with a fluence of ions along a line normal to the plane of the sensitive area, then the number of binary ones found after irradiation is equivalent to the number of upsets that have occurred. The upset cross section per BIT defined by

$$\sigma = \frac{\# \text{ Upsets}}{\text{Fluence}(\text{ions} / \text{cm}^2) * \text{BITS} / \text{part}} \quad \text{A-13)$$

depends on the LET of the incident ions as illustrated in Figure A.1-3. The approximate total area of the sensitive region in the plane of the part can be determined if the LET of the incident particles is sufficiently high that the upset cross section is saturated; i.e., $c(L) = c_{lim}$. This means that every particle passing through a sensitive region triggers an upset. If the flux is small so that each upset is due to a single ion, then the LET saturated cross section approximates the effective area of the sensitive region. Defining "a" to be the aspect ratio such that $l = aw$, the length and width of the sensitive region are given by

$$l = (\sigma_{lim} * a)^{0.5} \quad \text{A-14)$$

$$w = (\sigma_{lim} / a)^{0.5} \quad \text{A-15)$$

In the absence of additional information, it is usually a good approximation to assume that the sensitive region is a square area corresponding to an aspect ratio of one; however, according to the discussion on the sensitivity dependence of upset rate on aspect ratio given in Appendix B.1, the upset rate passes through a maximum for some value of the aspect ratio greater than or equal to one and subsequently decreases with increasing aspect ratio.

The upset rate is relatively insensitive to variation of the thickness for thin pancake shaped regions having a height $h \ll (l, w)$, as can be seen from the height sensitivity analysis given in Appendix B.1. Therefore, a rough guess for the height may be taken using available manufacturers' data for these cases. For example, this is about 0.5 microns for CMOS/SOS. In the event that the sensitive volume is not pancake shaped, ionizing particles will enter the region from the side introducing a more complex dependence of the upset rate on the depth. One of the methods referred to at the end of Section A.1.4 could be used to directly determine the critical charge and depth dimension; however, this is not necessary if it is desired to obtain only an upper

bound on the upset rate for the purpose of part qualification. To obtain an upper bound on the upset rate with respect to height, the height dimension should be chosen to be certainly less than the "actual" height as shown in the height sensitivity discussion in Appendix B.

The upset cross section defined by equation (A-13) may not have the well defined limit illustrated in Figure A.1-3. For these anomalous cases, the upset cross-section continues to increase as the LET increases. This occurs for parts having a high bit density when a single particle track of high LET trips several bit upsets, Kolasinski (1988). The heavy ion high LET particles have been shown to have large diameter tracks capable of inducing multiple upsets, Messenger (1982).

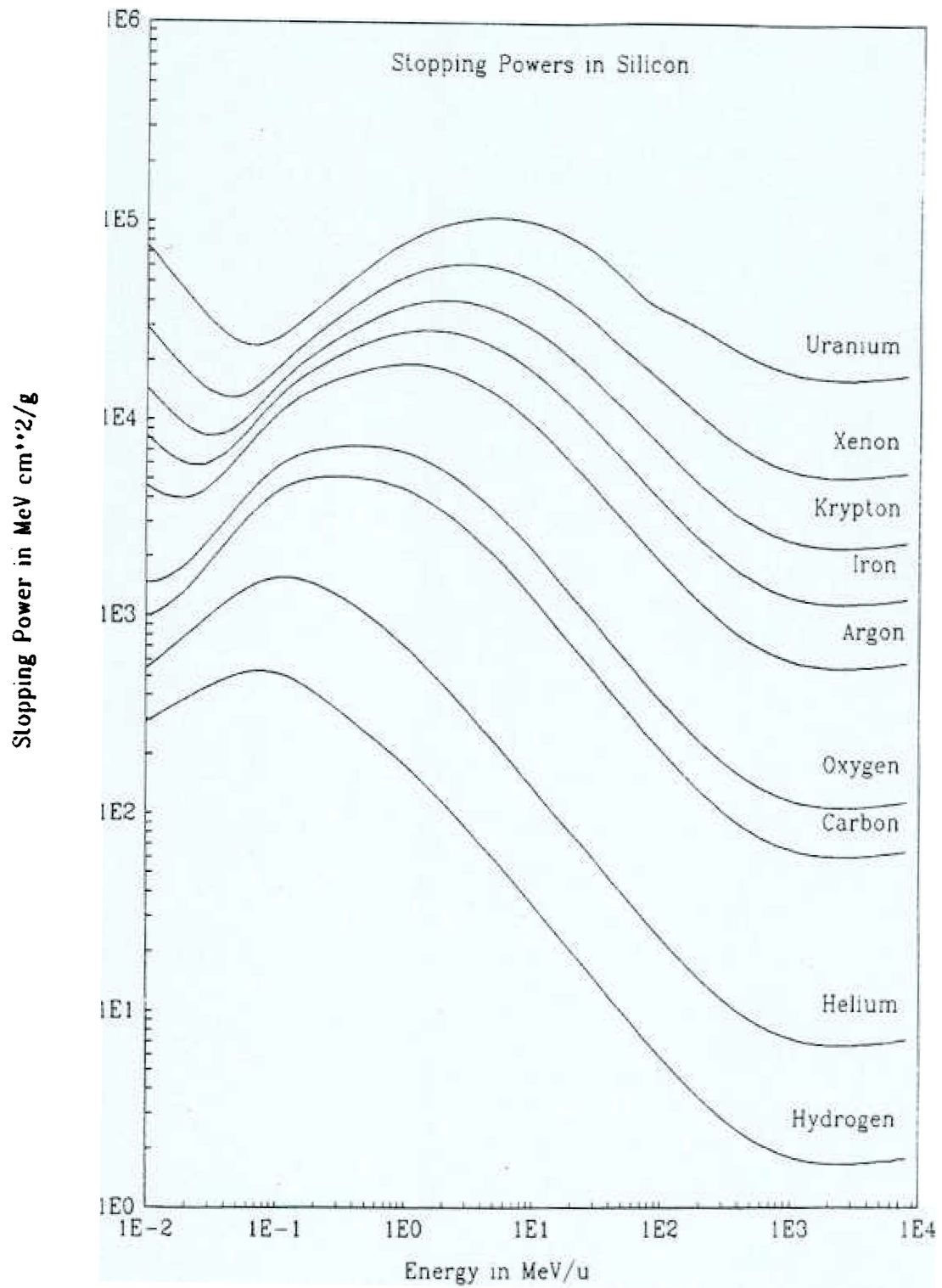


Figure A.1-1 The stopping power (or LET) versus energy per mass number for a variety of ions. Taken from Adams (1986).

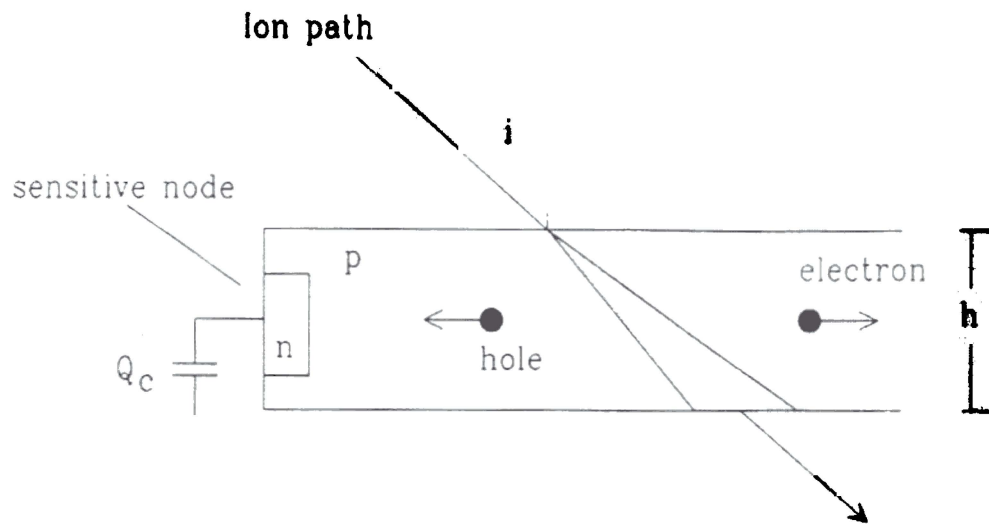


Figure A.1-2 Illustration of ion passing through the sensitive region of a semiconductor.

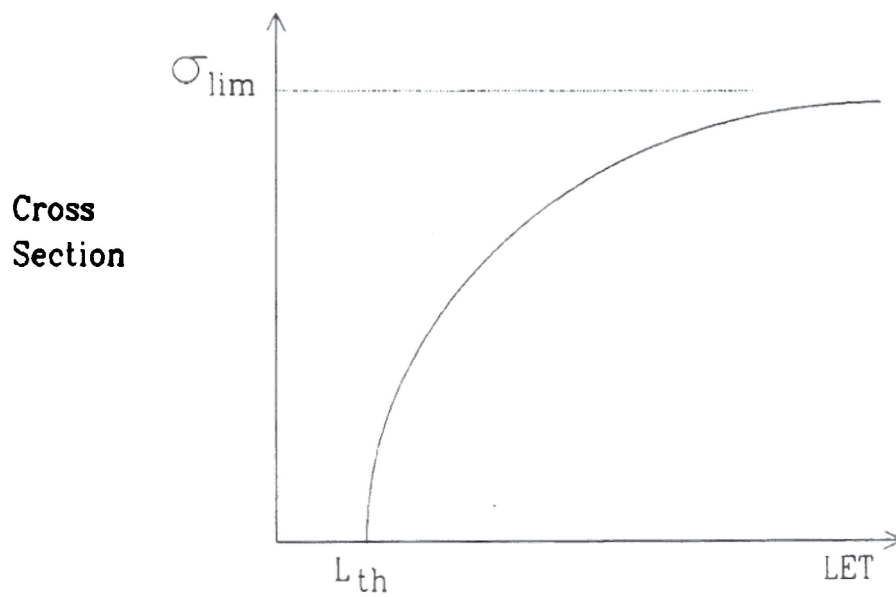


Figure A.1-3 Diagram illustrates the dependence of the upset cross section on the LET of the incoming ions.

A. 2 Greatest Upper Bound (GUB) on Upset Rate

As discussed in section A.1.5, the SEU rate of a part as determined by (A-10) is bounded with respect to variation in both aspect ratio and height. In view of the fact that only the threshold LET and cross section are available from accelerator experiments, it is highly desirable to have a simple general method of estimating an upper bound on the upset rate based only on accelerator data to use as an initial screening test to easily identify acceptable parts. An upper bound on the SEU rate satisfying these requirements exists, Chlouber (1988), and is given by

$$U_R < C_p \frac{\sigma_{lim}}{L_{th}^2} \quad \text{(A-16)}$$

wherein the coefficient C_p is given by

$$C_p = 4\pi \int_0^{L_{th}} \quad \text{(A-17)}$$

The result in (A-16) is similar to the "Single Event Upset Figure of Merit" formula due to Petersen (1983), the distinction being that the SEU rate coefficient is given exactly by the integral expression in (A-17). Together (A-16) and (A-17) constitute a rigorous upper bound on the SEU rate of a part with specified cross section and threshold LET. Figure A.2-1 illustrates the dependence of the coefficient C_p on the threshold LET for upset. Evaluation of C_p in the limit of high threshold LET for a 90 degree orbit corresponding to the environment given in Figure 2.2-2 yields

$$C_p(L_{th} = \text{infinite}) = 721 \text{ MeV}^2 \text{ cm}^2 \text{ mg}^{-2} \text{ day}^{-1} \quad \text{(A-18)}$$

which is in reasonable agreement with Petersen's numerical result obtained by integrating a power law curve fit of the LET spectrum.

The sensitivity analyses given in Appendix B illustrate for several examples how the GUB SEU rate formula in (A-16), along with (A-17) or (A-18), provides an upper limit on the single event upset rate. The use of the limiting value (A-18), however, may lead to an undesirable overestimate of the upset rate in the low threshold LET regime.

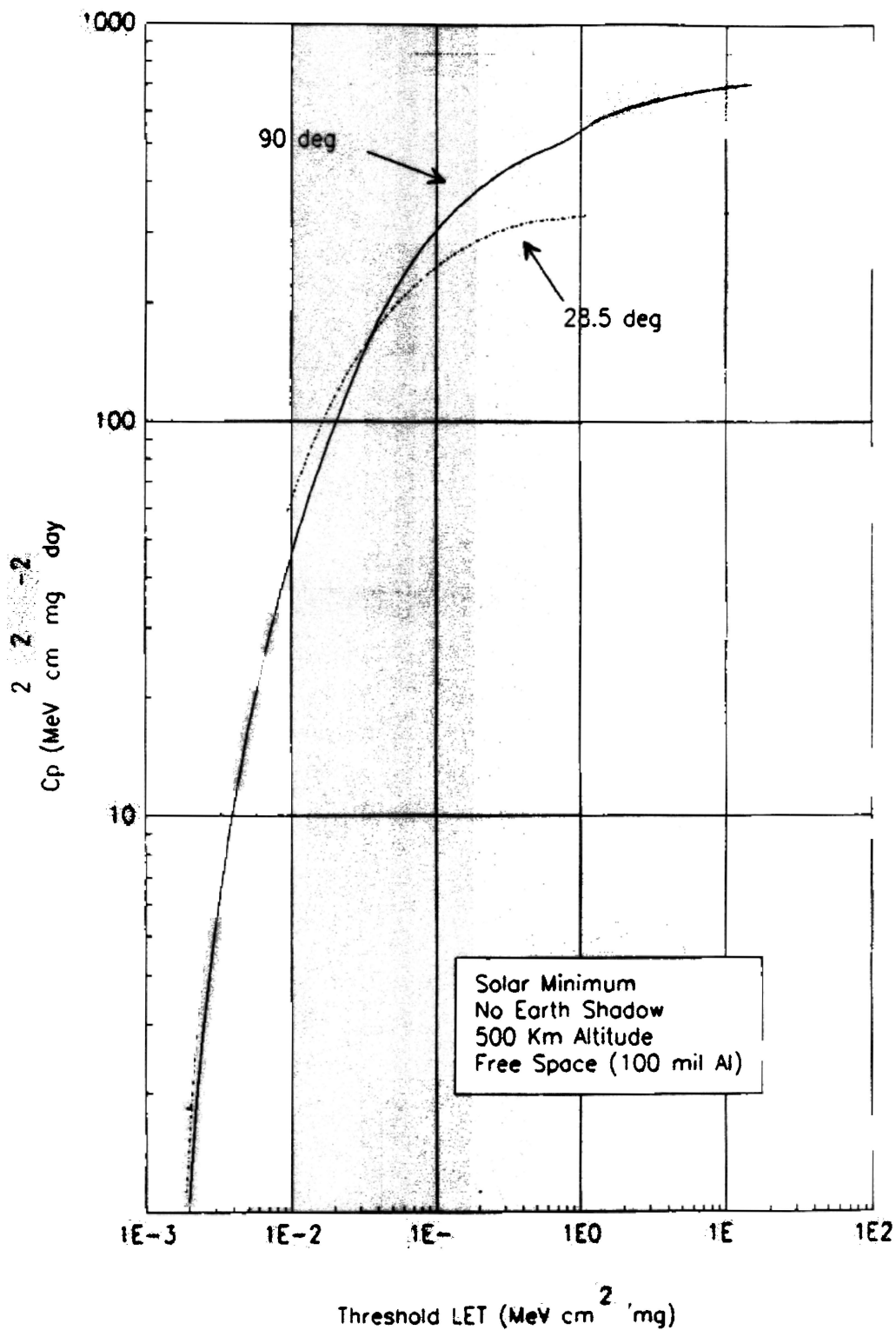


Figure A.2-1 Plot illustrating the dependence of error rate coefficient on the threshold LET.

A. 3 SEU Rate Computation

This section gives a method for computing an upper limit on the single event upset rate of a part

For initial screening Figure A.3-1 defines the steps required to determine the greatest upper bound (GUB) on the SEU rate: Experimental data for the threshold LET and the asymptotic cross section are obtained as defined in Appendix A.1. An upset rate coefficient is computed from (A-17) for the desired environment or obtained by interpolation of Table A.3-1 for a 90 degree orbit and 90% worst case interplanetary weather condition. The upper bound on the upset rate is given by (A-16).

L_{th} (MeV cm ² mg ⁻¹)	C_p (Mev ² cm ² mg ⁻² day ⁻¹)
0.01	45.9
0.1	302.6
1.0	538.2
10.0	697.6
100.0	721.4

Table A.3-1 SEU rate coefficient versus threshold LET for the 90 degree orbit and 90% worst case interplanetary weather condition.

If the GUB upset rate so obtained is acceptable, the part is qualified, if not, the part may still be acceptable in the case that the GUB upset rate formula has given too large an overestimate of the SEU rate. For this case Figure A.3-2 gives a secondary screening procedure which utilizes the known cross section and threshold LET and varies the height and aspect ratio of the sensitive region as illustrated in Figure B.1-2 to find the maximum possible physically realizable SEU rate.

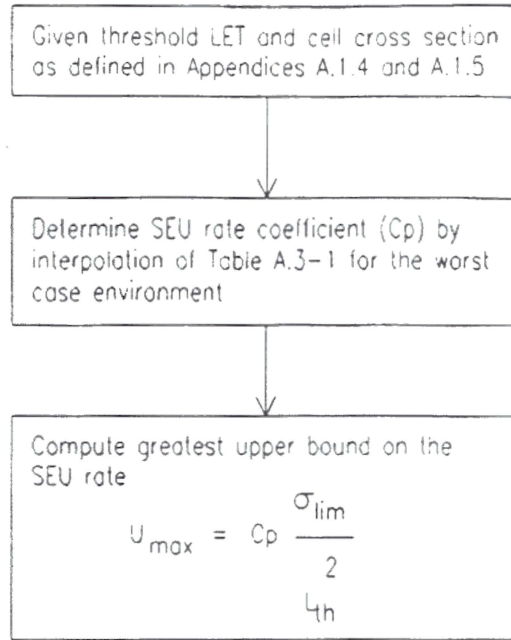


Figure A.3-1 Diagram illustrates the steps required to compute the greatest upper bound on the SEU rate.

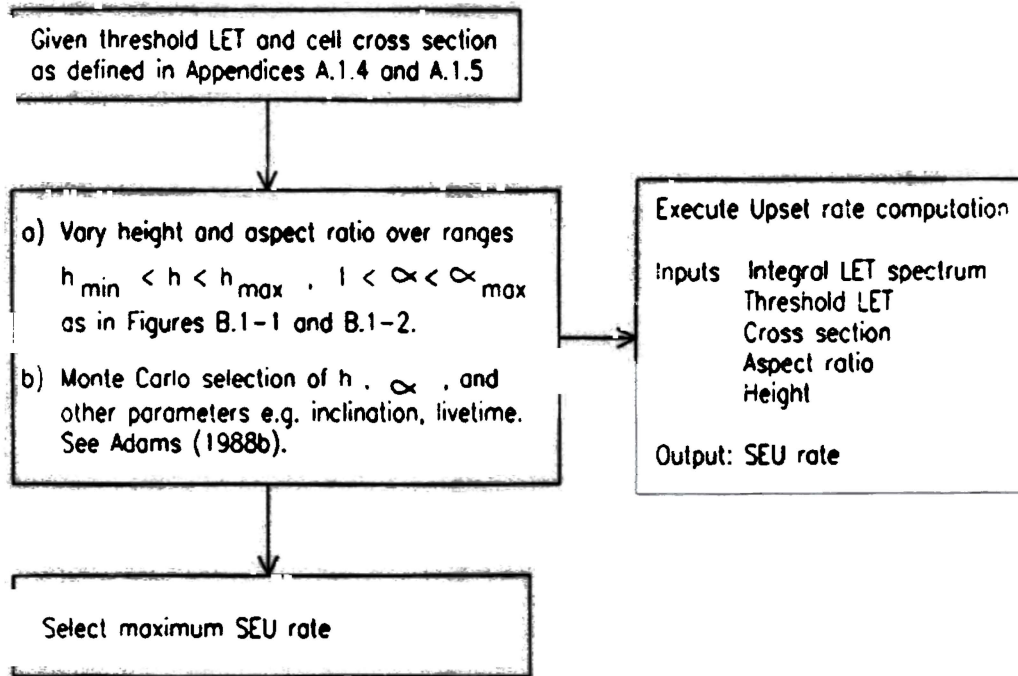


Figure A.3-2 Parametric analysis to determine the maximum physically realizable upset rate of a part.

A.4 Proton Induced Single Event Upset Calculation.

Unlike heavy ions, protons can seldom directly deposit enough charge to cause an upset. Proton interactions with nuclei within the device, however, can result in secondary particles capable of depositing enough charge in a sensitive volume to cause an upset. Not all devices will be susceptible to proton induced upsets. Upsets induced by protons may dominate in “softer” parts, but will become negligible in parts considered “hard” to testing with heavy ions.

Proton induced upsets will usually be only a fraction of those caused by heavy ions. In a few instances the proton induced upset rate may be higher than the heavy ion upset rate by a factor of 2 or 3, even 10 in extreme cases. If a part is soft and suspect of being very susceptible to proton induced upsets, further investigation and/or testing should be pursued. The following method and analysis can be used when it is desirable to have a complete and thorough calculation of a device’s upset rate.

The three basic mechanisms of interactions by which protons can cause upsets are: elastic scattering, alpha production, and fission reactions. Detailed descriptions of energy dependencies and probabilities for these reactions can be found in Bendel and Petersen (1983), Petersen (1981), and Guenzer et. al. (1979). These provide a comprehensive understanding of the physical phenomena, and the computations involved.

The cross-section for any of these reactions is small compared to the cross-section of the sensitive volume. The requirement that the reaction also occur within a short range of the sensitive volume further decreases the probability of proton induced upsets. These factors are counteracted by the high flux of trapped and solar flare protons. This high flux is enough to make protons a significant threat to some devices. In “hard” devices, protons will contribute very little, but the potential effects must not be routinely overlooked.

The important parameter used in calculating proton induced upsets is the apparent threshold, A , sometimes called the A parameter or Bendel’s A parameter, with units of MeV. This parameter is derived in a complicated way from experimental accelerator data on the proton energy versus upset rate curves. This parameter may be difficult to obtain, because of the limited testing that has been done with protons. No method presently exists for extrapolating heavy ion data into information about proton susceptibilities. The derivation of the apparent threshold can be found in Bendel and Petersen (1983). Once the apparent threshold is determined, the proton induced upset rate can be calculated for a given environment. The environments to be used are shown in Section 2.2.2. Plots of the upset rate versus apparent threshold, for the different environments, were calculated using the BENDEL codes of Adams et. al. (1986), and are given in Figure A.4.1 through A.4.4. The logarithmic dependence of these curves simplifies the upset rate calculation. For a known value of A , the following equations for upset rate – given in upsets/bit/day – can be used for each respective location, orbital inclination, and weather condition in Table A.4-1. The upset rate will be in upsets/bit/day, when the apparent threshold has units of MeV. Multiplying the upset rate/bit by the number of bits in the device will give the upset rate/device. Addition of

the heavy ion and proton induced upset rates gives the total upset rate for the device. This calculation need only be performed when it is deemed advantageous to use a very susceptible device. In the following table, quiet conditions refers to the 90% worst case environment for trapped and solar protons as described in Section 2, (quiet magnetosphere, and an interplanetary weather index = 3) as defined in the CREME codes by Adams (1986). The flare conditions are derived for the peak flux rates of an anomalously large solar flare of Aug. 4, 1972.

Internal Location, 28°, 57°, 90°	Quiet Conditions $UR = (1.2 \times 10^{13})A^{-14.2}$	(Fig. A.4-1) (upsets/bit/day)
Free Space Location, 28°, 57°, 90°	Quiet Conditions $UR = (3.3 \times 10^{13})A^{-14.3}$	(Fig. A.4-2) (upsets/bit/day)
Internal Location, 28° 57° 90°	Flare Conditions $UR = (1.5 \times 10^{13})A^{-14.3}$ $UR = (4.0 \times 10^{13})A^{-14.4}$ $UR = (2.2 \times 10^{15})A^{-14.5}$	(Fig. A.4-3) (upsets/bit/day) (upsets/bit/day) (upsets/bit/day)
Free Space Location, 28° 57° 90°	Flare Conditions $UR = (5.2 \times 10^{13})A^{-14.3}$ $UR = (5.3 \times 10^{15})A^{-14.5}$ $UR = (4.7 \times 10^{16})A^{-14.6}$	(Fig. A.4-4) (upsets/bit/day) (upsets/bit/day) (upsets/bit/day)

Table A.4-1 Equations for determining proton induced upset rates.

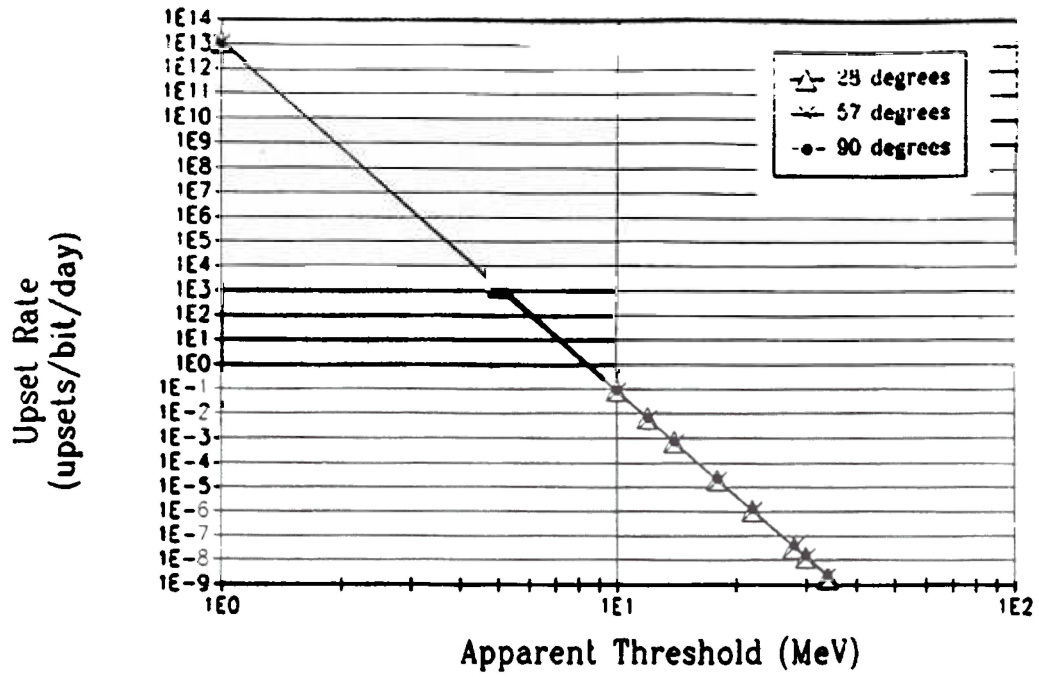


Figure A.4-1 Proton Induced Upset Rates, Quiet Conditions, Internal Location, at 28, 57, and 90 degrees

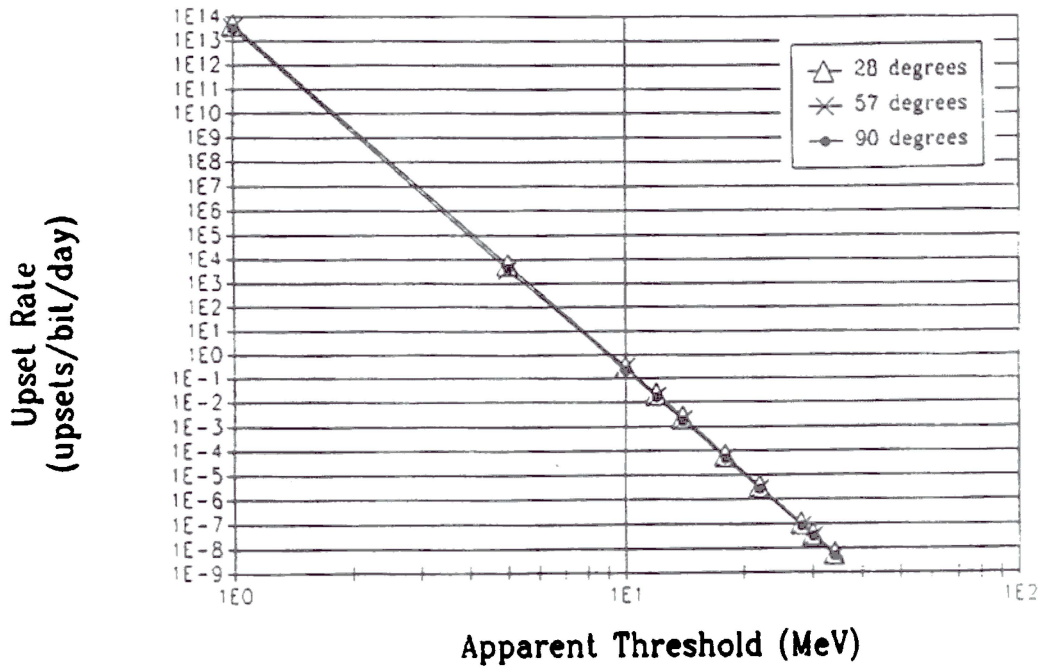


Figure A.4.2 Proton Induced Upset Rates, Quiet Conditions, Free Space Location, at 28, 57, and 90 degrees

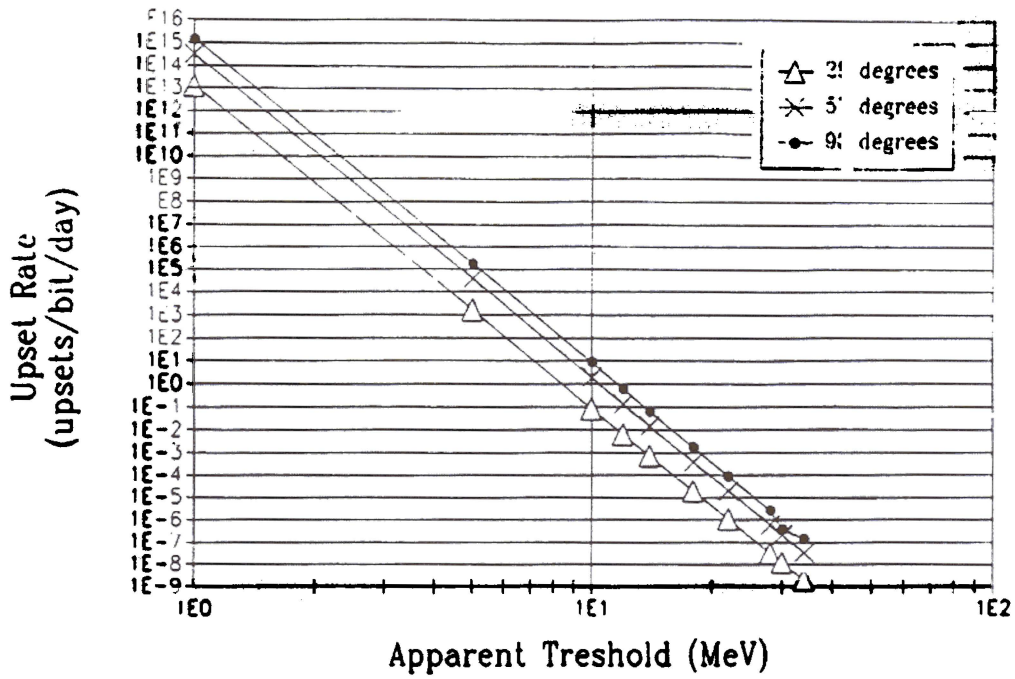


Figure A.4-3 Proton Induced Upset Rates, Flare Conditions, Internal Location, at 28, 57, and 90 degrees.

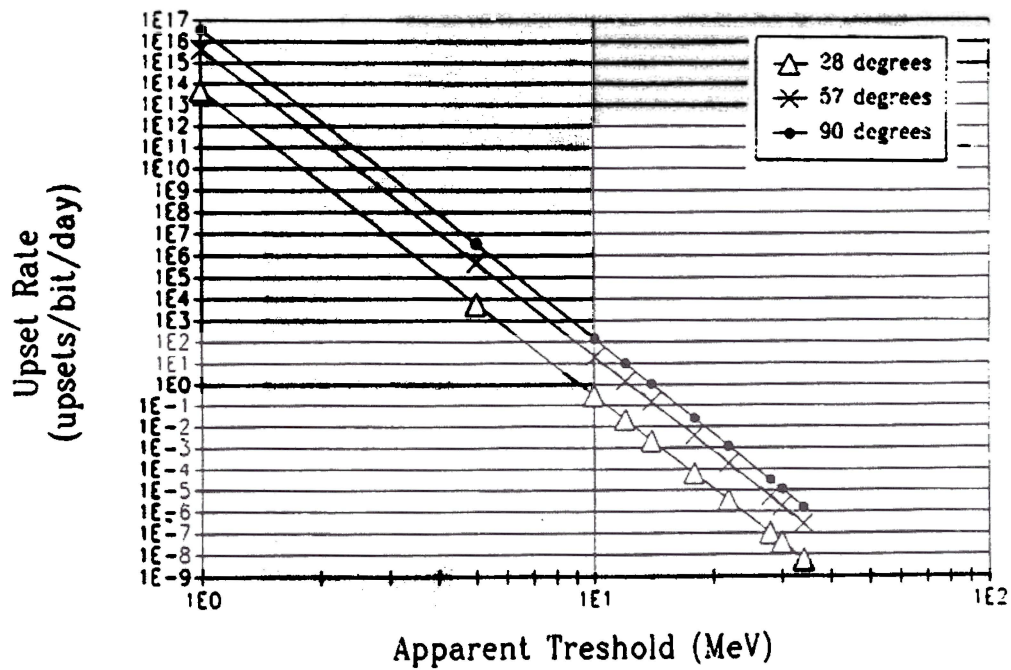


Figure A.4-4 Proton Induced Upset Rates, Flare Conditions, Free Space Location, at 28, 57, and 90 degrees.

A.5 Latchup

For latchup testing in the accelerator, the reference value of LET (L_{ref}) of the ionizing particles is chosen to be the peak stopping power of krypton ions ($L_{ref} \sim 36 \text{ MeV} \cdot \text{cm}^2/\text{mg}$) in the LET versus energy curves shown in Figure A.1-1. To understand this choice, we first note that the stopping power of krypton exceeds that for iron which represents the worst case of significance for the natural environment. As can be seen from examination of the integral LET spectrum shown in Figure 2.2-2, the flux of particles having a LET greater than the maximum stopping power of krypton is negligibly small (of order 10^{-8} particles/ $\text{m}^2/\text{ster}/\text{sec}$). This corresponds to roughly 10^{-4} particles/ cm^2 per year. If we assume that the sensitive parts onboard the Orbiter present an effective total cross sectional area of approximately 1000 cm^2 , then the chance that a particle with LET greater than L_{ref} for krypton will hit the sensitive area is once in approximately 10 years. Therefore the stopping power of krypton or an ion of equivalent LET represents a conservative upper bound on the maximum LET that stopping ions can deliver and is the basis for the presumption that parts may be tested for susceptibility to latchup in an accelerator using $36 \text{ MeV cm}^2/\text{mg}$ ions to simulate the highest LET particles expected in the orbital radiation environment.

The criterion for choosing the ion test fluence is based on the LET spectrum corresponding to the 90% worst case interplanetary weather condition ($M=3$) and the assumption that the GUB latchup rate is given by a relation analogous to (A-16)

$$L_R = C_p \frac{\sigma_{lim}}{L_{th}^2} \quad (\text{A-19})$$

wherein C_p is given by (A-18) and σ_{lim} and L_{th} now represent the cross section and threshold LET for latchup which are defined similarly to their SEU analogs. The mean time between latchups in the space environment is the reciprocal of the latchup rate

$$\text{MTBL} = 1/L_R \quad (\text{A-20})$$

If $L_{ref} \geq L_{th}$ and is large enough that it saturates the cross section (approximates the limiting value), then the required fluence of ions per latchup in the accelerator test is

$$f = 1/\sigma_{lim} = \frac{C_p \text{ MTBL}}{L_{th}^2} \quad (\text{A-21})$$

To obtain less than one chance in N of a latchup occurring in space, we can require that the mean time between latchups is equal to the factor (N) times the exposure time (T_e) to ionizing radiation

$$\text{MTBL} = N T_e \quad (\text{A-22})$$

Since L_{th} is unknown in the absence of additional experimental data, set $L_{ref} \sim L_{th}$ and substitute (A-22) in (A-21) to obtain

$$f \sim \frac{Cp N T_i}{L_{ref}^2} \quad (A-23)$$

Therefore, to achieve approximately one chance in 10,000 of latchup occurring during a space radiation exposure of 400 days (eight five day Orbiter missions per year for a ten year period), the fluence to test the part with is

$$2 \times 10^6 \text{ ions/cm}^2 \text{ per latchup} \quad (A-24)$$

Single event effects (SEU or latchup) can occur in space for parts that pass accelerator latchup tests because the space radiation spectrum is much more energetic than that of most accelerators – even though the LET used in the accelerator represents the space environment. In space, particles can traverse large shielding thicknesses and still have sufficient flux to cause SEE's. In accelerator tests, the beam penetration depth may be too small to reach the sensitive region due to large beam angle or a thick passivation layer. Also, few accelerator beams can penetrate a device from the side. However, the amount of ionization within the sensitive volume may be increased due to the particle's long path through the side of a device. In space, the sensitive region is easily reached and shielding actually increases the LET by slowing the particles. To illustrate this point, Figure A.5-1 shows the energy spectrum from a typical accelerator (300 MeV chlorine ions from a tandem Van de Graaff) and typical cosmic rays – hydrogen and iron ions for the 90% worst-case space environment for a 28.5 degree orbit. The accelerator spectrum has much higher flux but much lower energy than the cosmic rays of the space environment. The penetration depth of this accelerator beam is about 60 microns. Therefore, the accelerator is able to produce many SEE's in a reasonably short time for near normal incidence beams. On the other hand, the space ions are able to penetrate 5 inches of aluminum with little reduction in flux. Note from Figure A.5-1 that the iron spectrum is shifted toward lower energies with additional shielding. Figure A.1-1 shows a corresponding increase in the iron stopping power as the energy is decreased from about 10^3 to 1 MeV/nucleon. These differences between the space and test environments illustrate why parts may be qualified (to within certain limits) in a test environment, but not guaranteed immune in the space environment.

Figure A.5-2 shows the same data as in Figure A.5-1, but for a 90 degree orbit instead of a 28.5 degree orbit. Note the increased flux and spectrum breadth for the 90 degree orbit.

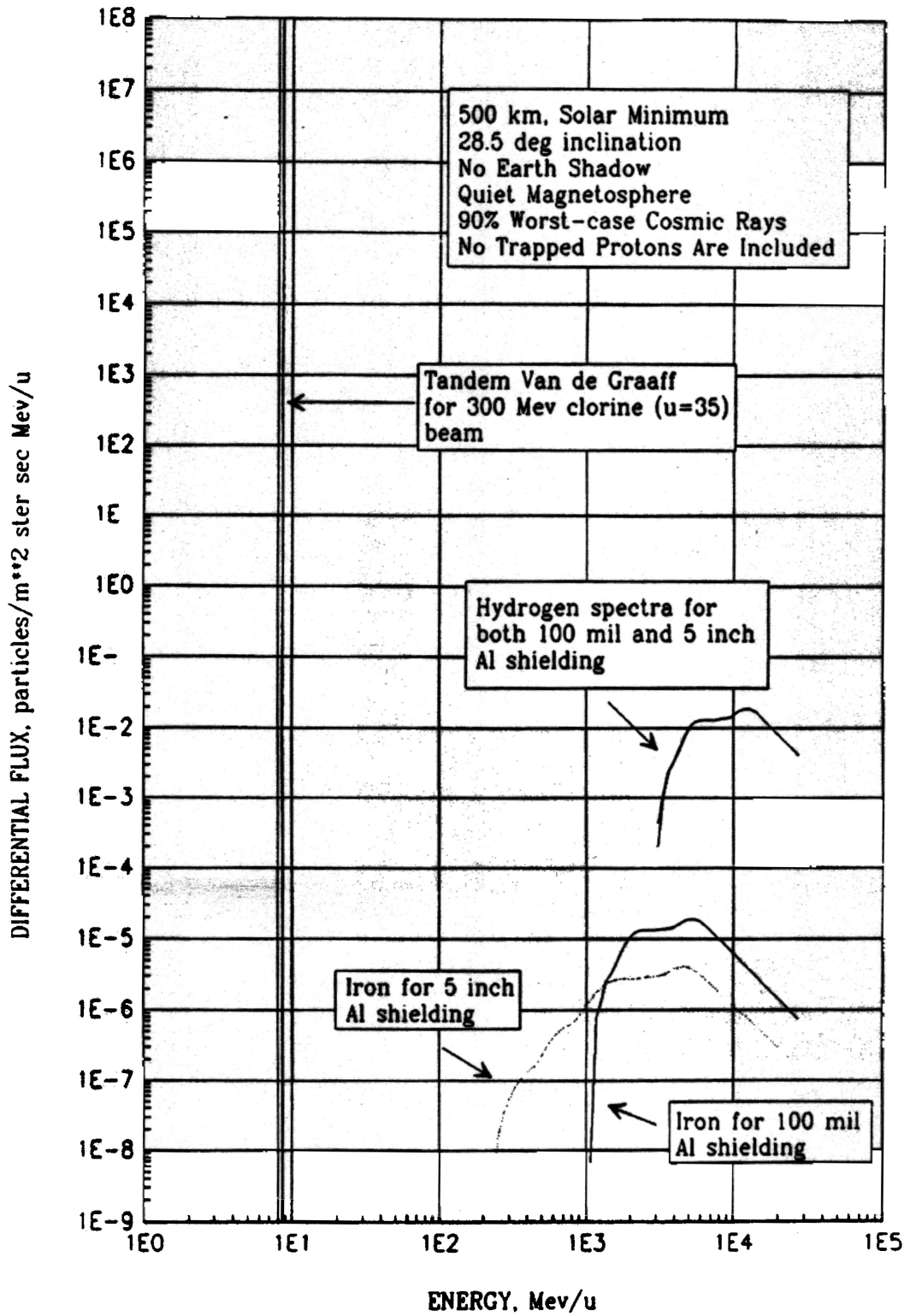


Figure A.5-1 Differential energy spectra for 90% worst-case (M=3) for 28.5 degree inclination orbit for hydrogen (u=1) and iron (u=56) cosmic rays for 100 mil Al and 5.0 inch Al shielding. Typical Tandem Van de Graaff spectra is shown for comparison.

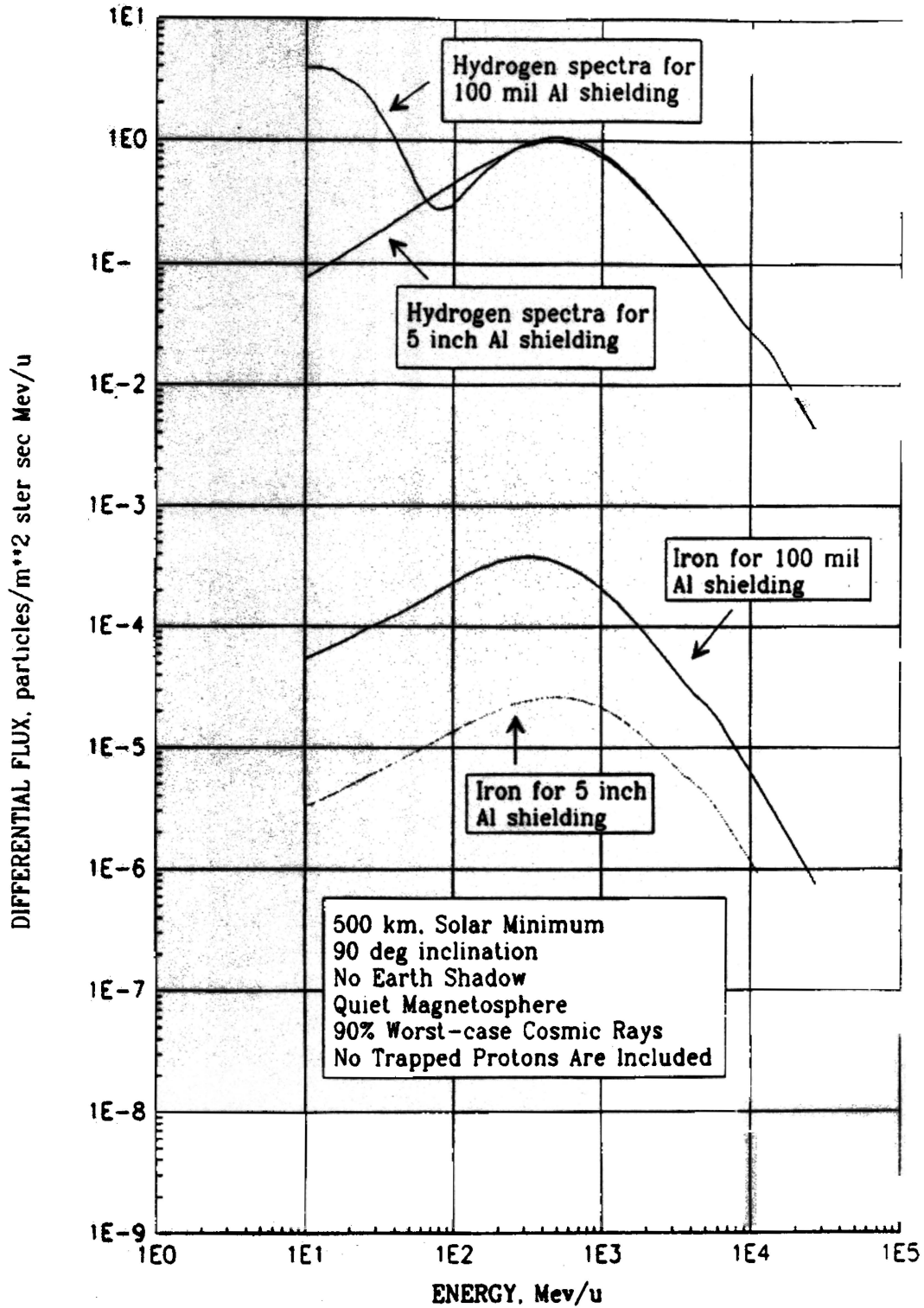


Figure A.5-2 Differential energy spectra for 90% worst-case (M=3) for 90 degree inclination orbit for hydrogen (u=1) and iron (u=56) cosmic rays for 100 mil Al and 5.0 inch Al shielding.

APPENDIX B

SINGLE EVENT EFFECT SENSITIVITY ANALYSIS

Accelerator tests can provide the threshold LET for producing an SEU and the limiting cross section per bit at large LET. However, in the absence of additional experimental tests, there is no information about the height of the sensitive volume or its aspect ratio. Also, there may be no information about how many sensitive volumes there really are per bit, or what their dimensions, thresholds, and live times are. That is, the measured threshold may be for the sensitive volume in each bit having the lowest threshold and the limiting cross section may be the sum of the limiting cross sections of each of the sensitive volumes per bit times the fractional live time for each of these sensitive volumes. In general, none of these details will be known.

In Appendix A, an upper limit on the SEU rate was given based only on accelerator test data. In this section we present supporting data for the upper limit given in (A-16) and consider the impact of additional device characteristics on the SEU rate.

The conclusions presented in this section constitute a brief synopsis of the work presented in Adams (1988) and Chlouber (1988).

Let's consider the dependence of the upset rate on each piece of missing information individually.

B.1 Height and Aspect Ratio

The overall dependence of the upset rate on the height is best understood from a physical point of view: Suppose that the threshold LET and bit cross section are fixed, for example, by measurements. It is evident from Eq. (A-12) that the critical charge, which measures the sensitivity to ionizing particles, decreases as h does; therefore, we expect that assuming a value of the height that is certainly less than the actual value, will overestimate the upset rate. This conclusion is supported by the data in Figure B.1-1 which plots the error rate as a function of the height of the sensitive region. As can be seen the "actual" error rate computed from Eq. (A-10) is less than the upper bound obtained from Eq. (A-16).

If we assume that the thickness of the depletion region in actual parts is in the range from 0.5 to 10 microns, it can be seen from Figure B.1-1 that the use of the upper bound in (A-16) overestimates the SEU rate of a 10 micron part by approximately two orders of magnitude.

The dependence of the upset rate on the aspect ratio can be understood as follows. For a finite rectangular region of fixed cross section, the upset rate must become vanishingly small for arbitrarily large aspect ratios. In this limit the sensitive region becomes a thin vertical slab. Since the LET that the ionizing particles can deliver is bounded, the only particles that will be effective in producing upsets will be those that are incident approximately in the plane defined

by the length(l) and height(h) of the sensitive region. However, for these particle paths, the path length distribution becomes arbitrarily small. Figure B.1-2 illustrates the dependence of the upset rate on aspect ratio. Note that the upset rate may first increase, pass through a maximum, and then decrease monotonically. The figure also shows that the value computed from the greatest upper bound formula in (A-16) is indeed an upper limit on the SEU rate for the example considered.

In practice the aspect ratio for a sensitive volume in a junction is usually in the interval $1 < a < 4$. For the example depicted in Figure B.1-2, this corresponds to a variation in the upset rate of approximately two percent for the $h = 1$ micron part. One can get large aspect ratios for bit lines, but if a bit line is sensitive to heavy ions, this will (presumably) be apparent in accelerator testing. In the accelerator test, bit line hits will cause all the bits on the line to flip. Figure B.1-2 also illustrates a secondary screening method that can be used to compute the maximum SEU rate of a part. Suppose, for example, that it is known that the minimum height of the sensitive region is 10 microns, then the maximum SEU rate occurs for an aspect ratio of approximately 10 as evident from the figure.

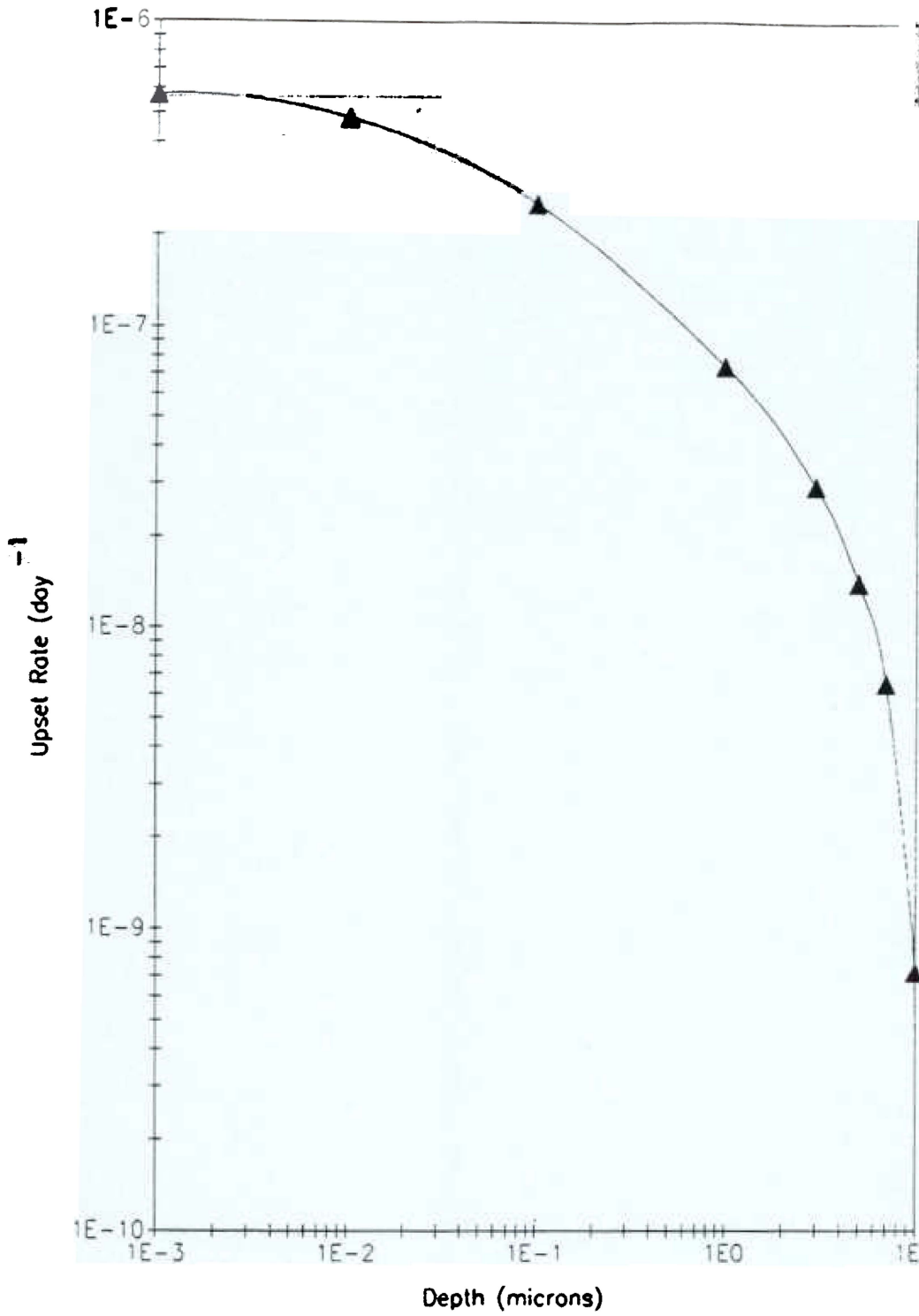


Figure B.1-1 Comparison of the actual and upper bound SEU rates versus depth. The threshold LET is 35000 MeV cm^{**2}/g and the cross section is 100 square microns.

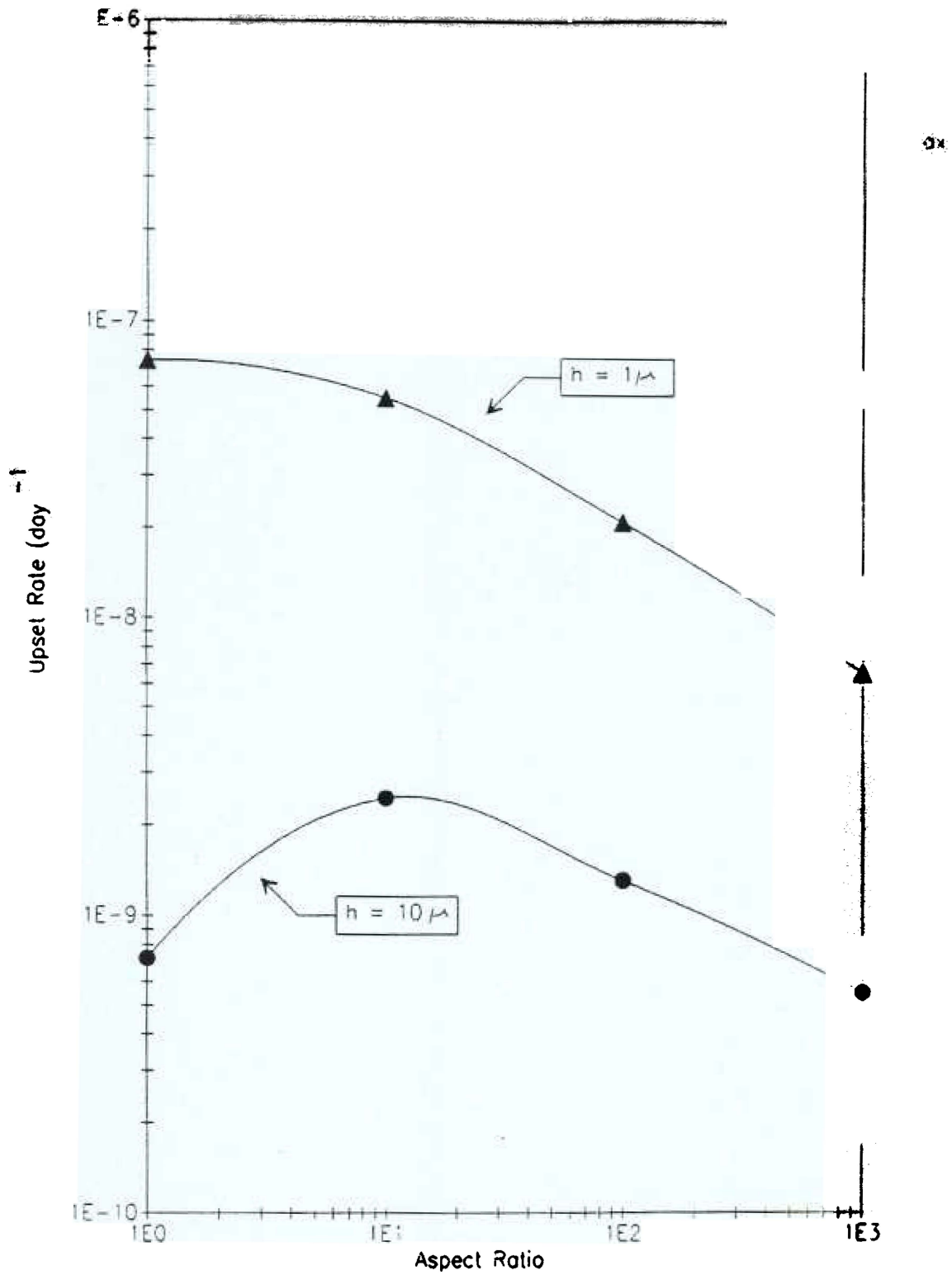


Figure B.1-2 Comparison of the actual and upper bound SEU rates versus aspect ratio. The threshold LET is 35000 MeV cm^{**2}/g silicon with a cross section of 100 square microns.

B.2 Fractional Live Time

Suppose that the sensitive volume is not sensitive all the time, but only some fraction, f , of “wall clock” time because of an internal clock cycle, or how it’s being used in a logic device. Failure to correct accelerator measurements for the device’s fractional live time can cause an underestimate of the SEE rate in space. This is explained by the following:

If the device is not “live” all the time during accelerator testing but a 100% live time is assumed, the limiting cross section will be underestimated. Now, the threshold LET will be measured correctly from the accelerator test. Therefore, if the sensitive volume’s height is estimated correctly, the critical charge will be calculated correctly. However, the underestimate of the sensitive volume will cause an underestimate of the long path lengths that are available to cosmic rays coming into the side of the sensitive device. These long paths lower the LET required to produce an upset and correspondingly increase the upset rate.

B.3 Multiple Sensitive Volumes per Bit

Suppose there is not one, but several sensitive junctions per bit in a device. Each junction will have its own sensitive volume and threshold. The accelerator tests will tell us only the lowest of these thresholds and a limiting cross section that is a sum of the cross sections of the individual sensitive volumes, weighted by their respective live times. Examples of this more complex SEU cross section dependence occur for bipolar IC’s and have been investigated by Zoutendyk, et. al. (1984).

As can be seen from (A-16), it is certainly conservative to assume that the lowest threshold applies to all sensitive volumes so that multiple volumes do not cause the SEU rate to increase. From the experimental test data for cross section versus LET, an upper bound on the upset rate will be obtained if we choose the minimum threshold LET and the maximum limiting cross section for all features and states of the device that ionizing radiation can probe.

APPENDIX C

PART RELIABILITY AND SINGLE EVENT EFFECT CALCULATION EXAMPLE

This section gives an example of the methods and calculations set forth by this document for determining, and comparing upset rates with hardware reliability. The part described does not represent any specific market device. This example uses a fictitious part developed from actual measurements where possible; therefore, the values are representative of values to be expected for such calculations. Any similarity between the example part and a specific market product is purely coincidental.

First the hardware reliability of the part, according to MIL-HDBK-217E, will be calculated. This reliability does not include the effects of ionizing radiation. Calculations for the effects of radiation will also be presented for comparison to the part hardware reliability. The part to be considered is an Electronically Programmable Logic Device (EPLD). The following reasonable assumptions are made about the EPLD:

- 1) B-2 quality level, representing that it is not fully compliant with requirements of Paragraph 1.2.1 of MIL-STD-883 and procured to government approved documentation including vendor's equivalent Class B requirements.
- 2) Operating temperature of 25°C
- 3) Operating voltage of 10 Volts
- 4) Approximately 2100 gates
- 5) 68 pins, DIPs, hermetic, glass sealed package
- 6) Space flight environment
- 7) New product or technology, has not been in continuous production for over four months.

The equation given in MIL-HDBK-217E for the failure rate, λ_p , for a part of this description is:

$$\lambda_p = P_Q [C_1 * P_T * P_V + C_2 * P_E] P_L$$

Using the definitions and tables in MIL-HDBK-217E, and the above assumptions results in the following values:

Quality factor	$P_Q = 5.0$
Temperature acceleration factor	$P_T = 0.1$
Voltage stress derating factor	$P_V = 1.0$
Circuit complexity factor	$C_1 = 0.24$
Package complexity factor	$C_2 = 0.048$

C-

Application environment factor	$P_E = 0.9$
Device learning factor	$P_L = 10.0$

Substitution of these values into the equation for failure rate yields

$$\lambda_p = 3.3 \text{ failures}/10^6 \text{ hrs}$$

To calculate the single event upset rate, U_R , and the latchup rate, L_R , due to radiation effects requires additional parameters. These parameters will be assumed as follows.

$$\text{Upset threshold, } LET_u = 12000 \text{ MeV cm}^2/\text{g}$$

$$\text{Upset cross section, } \sigma_u = 1.8 \times 10^{-4} \text{ cm}^2$$

$$\text{Latchup threshold, } LET_L = 14000 \text{ MeV cm}^2/\text{g}$$

$$\text{Latchup cross section, } \sigma_L = 7.0 \times 10^{-6} \text{ cm}^2$$

The upset rate will be calculated using the greatest upper bound (GUB) method described in Appendix A. Since the number of sensitive bits in the EPLD is unclear, it will be set equal to unity. The upper bound method gives for an upset rate:

$$U_R = 37 \text{ upsets}/10^6 \text{ hrs.}$$

The same method used for the upset rate calculation may be used for the latchup rate calculation by substituting in the latchup measurements. This yields a latchup rate of:

$$L_R = 1 \text{ latchups}/10^6 \text{ hrs.}$$

In summary

$$\lambda_p = 3.3 \text{ failures}/10^6 \text{ hrs.}$$

$$U_R = 37 \text{ upsets}/10^6 \text{ hrs.}$$

$$L_R = 1 \text{ latchups}/10^6 \text{ hrs.}$$

The above demonstrates the type of calculation that will serve as the foundation for determining the Effective MTBF. These calculations were performed only at the device level, and must be combined according to the standard handbook procedures described in MIL-STD-756B, to determine the MTBF at the LRU level. Ultimate satisfaction of the requirement given in section 1.4 will be determined after all hardware devices, architecture, and error correction codes are properly considered. The calculations demonstrated here are part of the overall process, but are not independently conclusive in themselves. Meaning, that an LRU may satisfy the requirements even if it is made up of devices which upset.

APPENDIX D

RADIATION ENVIRONMENT TABULATION

D.1 Trapped Radiation

Figures D.1-1 and D.1-2 define the orbit average trapped proton and electron radiation environments, respectively, at solar minimum for 28.5, 57.0, and 90.0 degree inclination circular orbits at 500 km altitude. Numerical values for this data are also provided in Tables D.1-1 and -2 since this data must be manually entered into the CREME program to model trapped proton and electron radiation.

These differential spectra were computed as described in Section 2 and were included in the integral LET spectra and the total dose calculations as stated throughout the text.

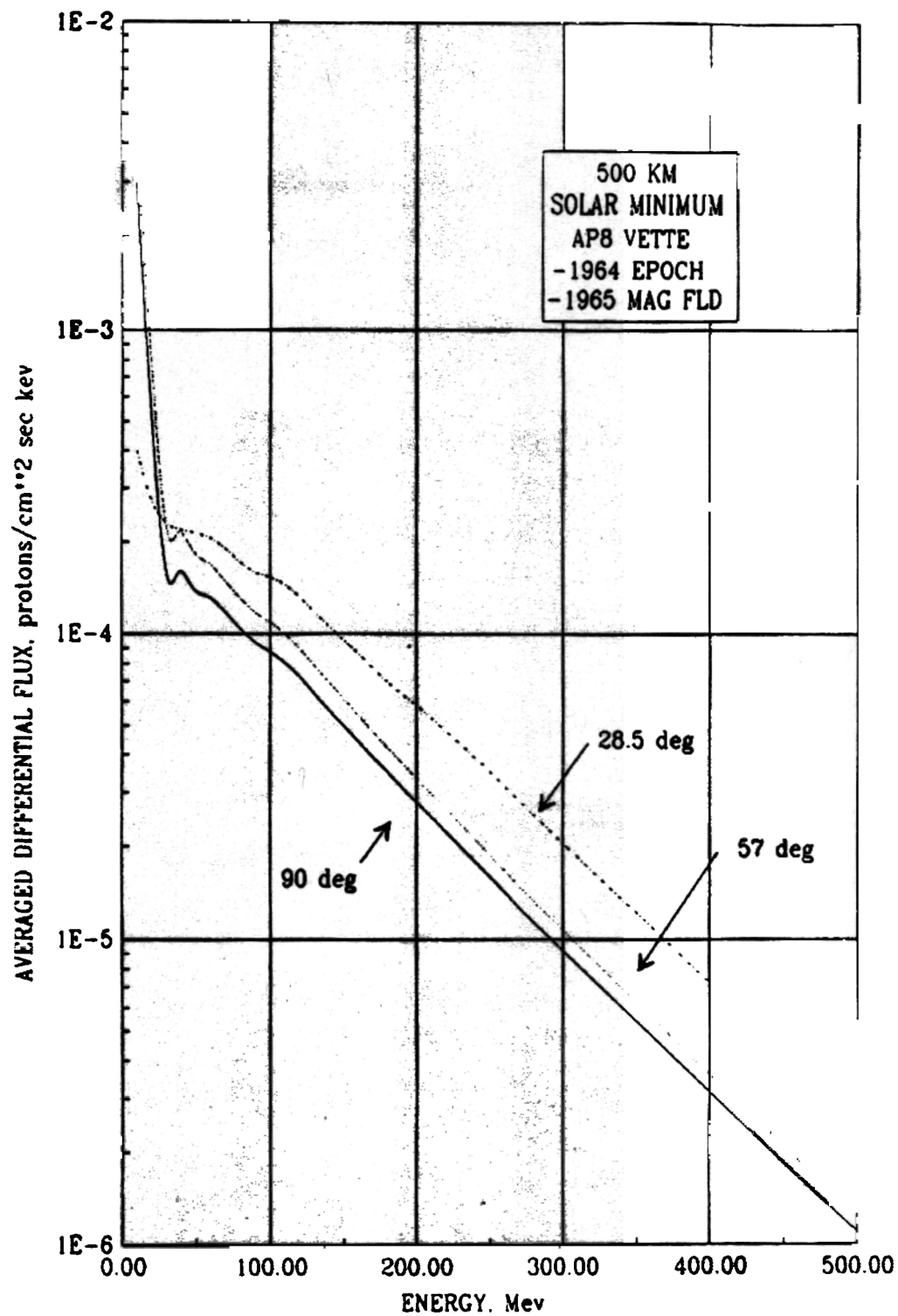


Figure D.1-1 Trapped proton spectra contribution to radiation environment (unshielded). Orbit averaged for 28.5, 57, and 90 degree orbits passing through the South Atlantic Anomaly.

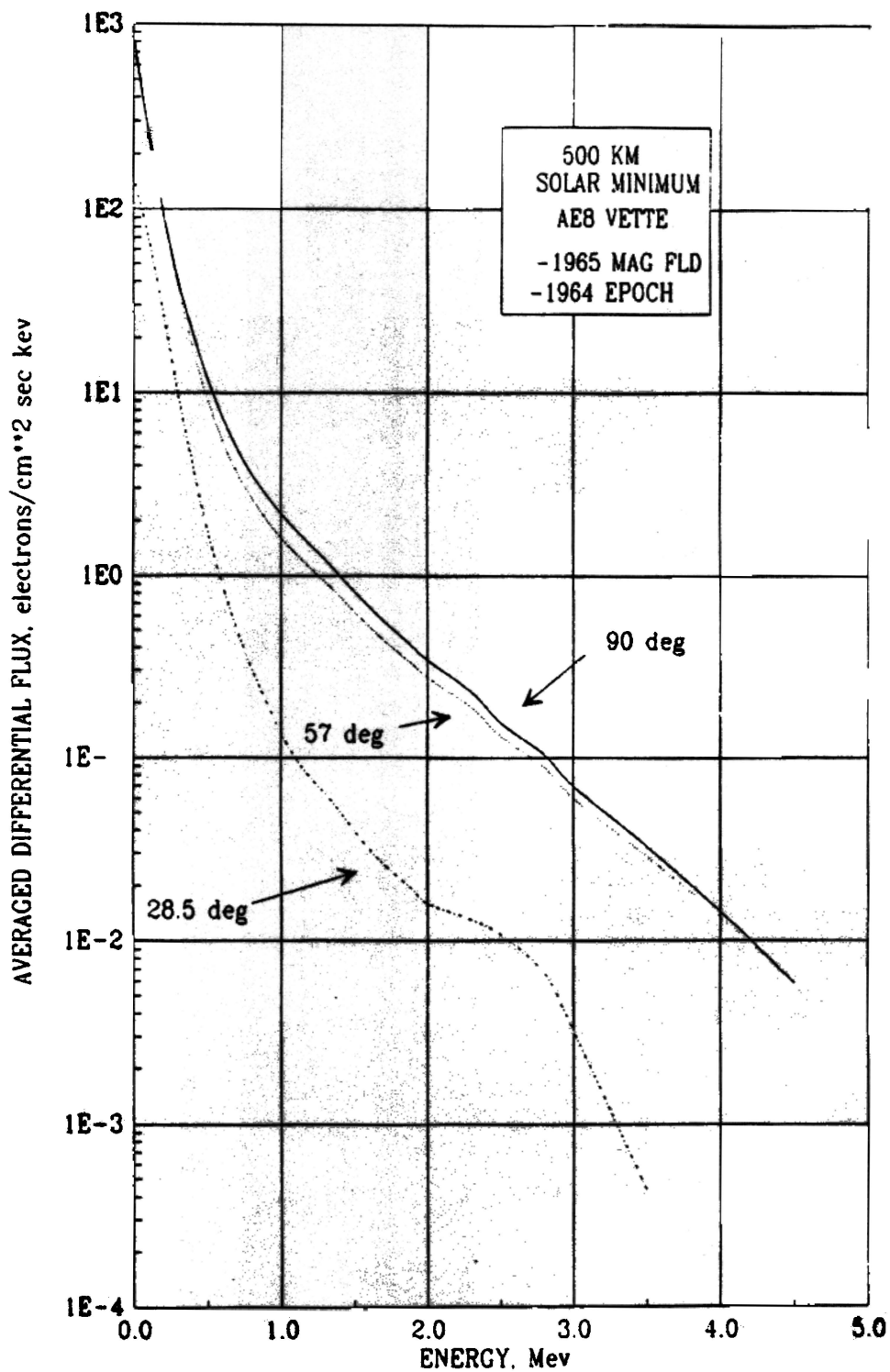


Figure D.1-2 Trapped electron spectra contribution to radiation environment (unshielded). Orbit averaged for 28.5, 57, and 90 degree orbits passing through the South Atlantic Anomaly.

ENERGY, MeV	DIFFERENTIAL FLUX, protons/cm**2 sec kev		
	28.5 deg	57 deg	90 deg
0.10000E+02	0.40000E-03	0.45300E-02	0.30100E-02
0.20000E+02	0.27300E-03	0.71400E-03	0.48600E-03
0.30000E+02	0.23000E-03	0.22000E-03	0.15700E-03
0.40000E+02	0.21900E-03	0.21500E-03	0.16000E-03
0.50000E+02	0.21300E-03	0.18100E-03	0.13800E-03
0.60000E+02	0.20500E-03	0.16800E-03	0.13100E-03
0.70000E+02	0.18900E-03	0.14800E-03	0.11700E-03
0.80000E+02	0.17100E-03	0.13100E-03	0.10400E-03
0.90000E+02	0.15900E-03	0.11700E-03	0.93900E-04
0.10000E+03	0.15300E-03	0.10900E-03	0.87300E-04
0.11000E+03	0.14500E-03	0.10000E-03	0.80400E-04
0.12000E+03	0.13200E-03	0.89600E-04	0.72100E-04
0.13000E+03	0.11800E-03	0.78800E-04	0.63700E-04
0.14000E+03	0.10600E-03	0.69300E-04	0.56200E-04
0.15000E+03	0.95500E-04	0.61100E-04	0.49900E-04
0.16000E+03	0.85800E-04	0.53900E-04	0.44200E-04
0.17000E+03	0.77100E-04	0.47700E-04	0.39200E-04
0.18000E+03	0.69400E-04	0.42200E-04	0.35000E-04
0.19000E+03	0.63100E-04	0.37500E-04	0.31100E-04
0.20000E+03	0.58000E-04	0.33400E-04	0.27800E-04
0.22500E+03	0.45400E-04	0.25000E-04	0.21100E-04
0.25000E+03	0.35000E-04	0.18800E-04	0.16000E-04
0.27500E+03	0.26700E-04	0.14100E-04	0.12000E-04
0.30000E+03	0.20500E-04	0.10700E-04	0.91800E-05
0.35000E+03	0.12200E-04	0.61900E-05	0.53700E-05
0.40000E+03	0.72100E-05	0.35900E-05	0.31500E-05
0.45000E+03	0.43100E-05	0.20800E-05	0.18500E-05
0.50000E+03	0.25700E-05	0.12300E-05	0.11000E-05

Table D.1-1 Tabulation of data plotted in Figure D.1-1. Trapped proton spectra contribution to radiation environment (unshielded) Orbit averaged for 28.5, 57, and 90 degree orbits passing through the South Atlantic Anomaly

ENERGY, MeV	DIFFERENTIAL FLUX, electrons/cm**2 sec kev		
	28.5 deg	57 deg	90 deg
0.10000E-01	0.13900E+03	0.67600E+03	0.78900E+03
0.10000E+00	0.68400E+02	0.25800E+03	0.26500E+03
0.20000E+00	0.26900E+02	0.93600E+02	0.96300E+02
0.30000E+00	0.98700E+01	0.36900E+02	0.41100E+02
0.40000E+00	0.39800E+01	0.17100E+02	0.20800E+02
0.50000E+00	0.17700E+01	0.90400E+01	0.11800E+02
0.60000E+00	0.89400E+00	0.54100E+01	0.72900E+01
0.70000E+00	0.50600E+00	0.36300E+01	0.49500E+01
0.80000E+00	0.31000E+00	0.26400E+01	0.36000E+01
0.90000E+00	0.20100E+00	0.20100E+01	0.27400E+01
0.10000E+01	0.13700E+00	0.16100E+01	0.21800E+01
0.11000E+01	0.98700E-01	0.13200E+01	0.17700E+01
0.12000E+01	0.77400E-01	0.11000E+01	0.14700E+01
0.13000E+01	0.63400E-01	0.92200E+00	0.12200E+01
0.14000E+01	0.50900E-01	0.76700E+00	0.10000E+01
0.15000E+01	0.39800E-01	0.63200E+00	0.81700E+00
0.16000E+01	0.31600E-01	0.52300E+00	0.67100E+00
0.17000E+01	0.26200E-01	0.44200E+00	0.56100E+00
0.18000E+01	0.22200E-01	0.37600E+00	0.47500E+00
0.19000E+01	0.18900E-01	0.32200E+00	0.40200E+00
0.20000E+01	0.15900E-01	0.27400E+00	0.34000E+00
0.23000E+01	0.13000E-01	0.18900E+00	0.22900E+00
0.25000E+01	0.10700E-01	0.13100E+00	0.15500E+00
0.28000E+01	0.66200E-02	0.88800E-01	0.10400E+00
0.30000E+01	0.31700E-02	0.59700E-01	0.69400E-01
0.35000E+01	0.43600E-03	0.28900E-01	0.32600E-01
0.40000E+01		0.13500E-01	0.14500E-01
0.45000E+01		0.58100E-02	0.58800E-02
0.50000E+01		0.21100E-02	0.20000E-02
0.60000E+01		0.92800E-04	0.82300E-04

Table D.1-2 Tabulation of data plotted in Figure D.1-2. Trapped electron spectra contribution to radiation environment (unshielded). Orbit averaged for 28.5, 57, and 90 deg orbits passing through the South Atlantic Anomaly

APPENDIX E

ORBITER AVIONICS RADIATION SPECIFICATION

*WORKING GROUP MEMBERS, 1987

Chairman: Frank Littleton (VG)

NAME	PHONE:
Jim Adams, Code 4154.2 Naval Research Lab 4555 Overlook Ave. Washington, DC 20375-5000	(202) 767-2747 FAX: (202) 767-6473
Bill Atwell, SN32 Bldg. 261, Rm. 128 NASA/JSC Houston, TX 77058	(713) 483-6194
David Beverly, NB5 Bldg. 45, Rm. 631 NASA/JSC Houston, Texas 77058	(713) 483-4202
Jim Blandford Consultant 10 Cerrito Irvine, CA 92715	(714) 854-9044
Dean Chlouber MDAC-ES 16055 Space Center Houston, TX 77062	(713) 280-1754 FAX: (713) 280-1583
Michael Defrancis, HS02 Boeing P.O. Box 58747 Houston, TX 77058	(713) 280-7581
K.W. Dunn NASA/JSC Houston, TX 77058	(713) 483-8367
David Fitts, VP 12 Bldg. 1, Rm. 624 NASA/JSC Houston, TX 77058	(713) 483-0123

E-

Note: Member's address, office code, and phone numbers may be out of date.

Alva Hardy, SN3
Bldg. 261, Rm. 127
NASA/JSC
Houston, TX 77058

(713) 483-6189

Harry Horii
FB10, Dept. 292
Rockwell International
12214 Lakewood
Downey, CA 90241

(213) 922-3441
FAX: (213) 922-0542, 3

Sherra Kerns
P.O. Box 108, Sta. B
Vanderbilt University
Nashville, TN 37235

(615) 322-2771

Ralph Lawton
MDAC-ES
16055 Space Center
Houston, TX 77062

(713) 280-1576
FAX: (713) 280-1583

Frank Littleton, VG
Bldg. 1, Rm. 661B
NASA/JSC
Houston, TX 77058

(713) 483-2744

Gino Manzo
IBM
9500 Godwin Drive
Manassas, VA 22110

(703) 367-3418
FAX: (703) 367-4259

Dan Marlowe
Bldg. 1
NASA/JSC
Houston, TX 77058

(713) 483-0951

Cecilia Matuschek
Rockwell Anaheim
Anaheim, CA

(714) 762-0706

Charles Murphy
Building 157
TRW Components International Inc.
19951 Mariner Avenue
Torrance, CA 90503

(213) 214-5637 Telex: 674476
FAX: (213) 214-5637

Pat O'Neill
MDAC-ES
16055 Space Center
Houston, TX 77062

(713) 280-1668
FAX: (713) 280-1583

Karl Pfitzer
McDonnell Douglas
5301 Bolsa Ave.
Huntington Beach, CA 92647-2048

(714) 896-3231
FAX: (714) 896-1313

Patrick Pilola, NB5
NASA/JSC
Houston, TX 77058

(713) 483-4203
FAX: (713) 483-2080

Jim Pollock
MDAC-ES
16055 Space Center
Houston, TX 77062

(713) 280-1500 (x3092)
FAX: (713) 280-1583

Barry Posey
IBM
9500 Godwin Drive
Manassas, VA 22110

(703) 367-1686
FAX: (703) 367-4259

John Rector, WG2
Bldg. 1, Rm. 326
NASA/JSC
Houston, TX 77058

(713) 483-0764

Richard Roddy
Honeywell Inc.
Box 52199
Phoenix, AZ 85072

(602) 561-3393
FAX: (602) 561-3200

Tom Scott, MS/20/024
IBM
9500 Godwin Drive
Manassas, VA 22110

(703) 367-6169
FAX: (703) 367-4259

Paul Sollock, EH4
Bldg. 16A, Rm. 2152C
NASA/JSC
Houston, TX 77058

(713) 483-8356

E.H. 'Suds' Sudduth FB 14 Rockwell International 12214 Lakewood Downey, CA 90241	(213) 922-3068
Vincent Valloppillil, NB5 Bldg. 45 NASA/JSC Houston, Texas 77058	(713) 483-6248
Orlando Van Gunten Lab for Physical Sciences 4928 College Ave. College Park, MD 20740	(301) 277-4190
Ray Volk Honeywell Inc. Box 52199 Phoenix, AZ 85072	(602) 561-3155 FAX: (602) 561-3200
Al Waskiewicz, HB11 Rockwell International 3370 Miraloma Ave. Anaheim, CA 92803	(714) 762-2108
Art Wong Honeywell Inc. Box 52199 Phoenix, AZ 85072	(602) 561-3126 FAX: (602) 561-3200
Chung-Ho Wong, FB2O 12214 Lakewood Blvd. Downey, CA 90214	(213) 922-9503 FAX: (213) 922-2015
Bill Yucker McDonnell Douglas 5301 Bolsa Ave. Huntington Beach, CA 92647-2048	(714) 896-3833 FAX: (714) 896-1313

**APPENDIX F
GLOSSARY/ACRONYMS**

amu	Atomic mass unit, a unit of mass equal to $.65979 \times 10^{-24}$ g
bremsstrahlung radiation	Electromagnetic radiation emitted when a charged particle is accelerated by the coulomb field of a nucleus, most commonly X- or Gamma rays from relativistic electrons decelerating in a solid.
Cerenkov radiation	Ultraviolet and visible light emitted when a charged particle passes through a transparent dielectric medium with a relative speed exceeding the phase velocity of light in the medium.
cm	centimeter
differential spectrum	Flux of particles per unit interval in either energy or linear energy transfer (LET).
displacement	Applied to radiation: Effect inducing change in the position of atoms in a crystal lattice or solid. Accumulated or total energy absorbed in some material or medium due to radiation, in units of rads [1 rad (material) = 100 ergs/g in material].
equipment	Any electrical, electronic, or electromechanical device, or collection of items, intended to operate as an individual unit and perform a singular function.
fluence	Total, or time integrated, flux.
flux	Rate of flow of particles through a unit area per unit time. (Can be integral or differential.)
g	gram Government Furnished Equipment Greatest upper bound
integral spectrum	The total flux of all particles above a given energy or LET value.
Latchup	A loss of functionality which results when the output is locked at or near a supply or ground voltage and is not affected by controlled input changes. The device is effectively disabled and can be enabled only by the removal and re-application of supply power. Linear Energy Transfer. The deposition of energy per unit length in material by a charged particle measured in units MeV cm ² /g. Alternative units are defined by: LET(MeV/cm) = density(g/cm ³) * LET (MeV cm ² /g)

live time	Fraction of time device is in sensitive state Line Replaceable Unit.
m	meter Million electron-Volt
micron	1×10^{-6} meters 1×10^{-3} inches
	Mean Time Between Failures
OMS	Orbital Maneuvering System
permanent damage	Permanent failure of a semiconducting part that occurs when an ionizing particle causes a short circuit through the gate oxide insulation region.
rad (material)	A measure of dose. Radiation energy per unit mass imparted to some material or medium; 1 rad (material) = 100 ergs/g in material (E.g., rads (silicon))
sec	second Single event effect. A term meaning latchup or single event upset Single event upset. An unintentional change in the state of a digital device, resulting in erroneous data or control. The change of state is not permanent in that complete functionality can be restored by reprogramming. steradian
stopping power	The energy loss per unit length by a charged particle measured in MeV/cm or MeV cm ² /g. See also Linear Energy Transfer.
system	A composite of equipment, subsystems, skills, and techniques capable of performing or supporting an operational role. A complete system includes related facilities, equipment, subsystems, materials, services, and personnel required for its operation to the degree that it can be considered self-sufficient within its operational or support environment.
u	Mass number. Mass of a particle measured in amu's (e.g., u is 56 for iron)
z	Atomic number, equal to the number of protons in the nucleus (e.g., z is 26 for iron)